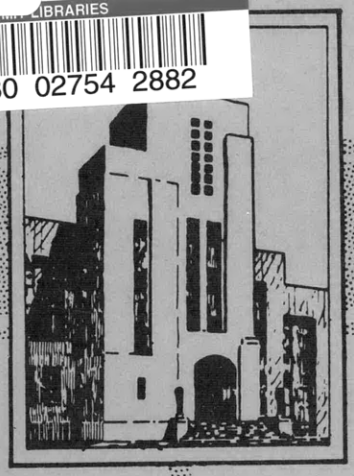

DEPARTMENT OF THE NAVY

DAVID TAYLOR MODEL BASIN

HYDROMECHANICS

○

AERODYNAMICS

○

STRUCTURAL MECHANICS

○

APPLIED MATHEMATICS

A CONTROL-SURFACE FLUTTER STUDY IN THE FIELD OF NAVAL ARCHITECTURE

by

R.T. McGoldrick and D.A. Jewell

STRUCTURAL MECHANICS LABORATORY
and
HYDROMECHANICS LABORATORY

RESEARCH AND DEVELOPMENT REPORT

September 1959 Report 1222

PRNC-TMB-648 (Rev. 3-58)

A CONTROL-SURFACE FLUTTER STUDY IN THE FIELD OF NAVAL ARCHITECTURE

by

R.T. McGoldrick and D.A. Jewell

September 1959

Report 1222
NS 715-090

TABLE OF CONTENTS

LIST OF FIGURES

LIST OF TABLES

NOTATION

A	Lift constant of hydrofoil (lift force per unit attack angle per unit velocity squared)
A_0, A_1, A_2, A_3	Coefficients in frequency equation
b	Semichord length of foil
C	Linearized damping constant for the translational degree of freedom at zero velocity
C_k	Theodorsen's function of reduced frequency appearing in the expressions for oscillatory lift and moment
c	Linearized damping constant for the rotational degree of freedom at zero velocity
D	Routh discriminant of oscillatory stability
DR	Damping ratio on the basis of unity for critical damping (logarithmic decrement observed divided by 2π)
F_L	Oscillatory lift force less the added mass effect
f	Frequency
h	Distance from the axis to the center of gravity (c.g.) of the rotating assembly, based on mass plus added mass (positive if c.g. is downstream)
I	Effective mass moment of inertia of the rotating assembly with respect to its axis, including the added mass moment of inertia of the hydrofoil
K	Spring constant of the rotational degree of freedom
L	Distance of the center of lift from the axis of rotation (positive if the center of lift is upstream)
l	Length of the hydrofoil
M	Mass of the system which vibrates only in translation
M_θ	Oscillatory hydrodynamic moment about the axis of rotation less the added mass effect
m	Mass of the hydrofoil including the mass of the entire assembly that rotates with it and the added mass in translation
P_0	Effective force on the nonrotating element
S	Hydrofoil speed
Y	Displacement of the control-surface axis normal to the flow and to the axis of rotation from the equilibrium position
$Y_{c.g.}$	Displacement of the center of gravity of the rotating assembly in the Y-direction
Y_0	Single amplitude of vibration in Y-direction

α	Effective angle of attack of foil from the equilibrium position
α_0	Preset angle of attack of foil
θ	Rotational displacement of the control surface from the equilibrium position
θ_0	Single amplitude of rotational vibration
λ	Complex circular frequency of vibration
μ	Real part of complex circular frequency indicating the degree of damping
ν	Kinematic viscosity of fluid
ρ	Mass density of fluid
ϕ	Phase angle (defined on page 27)
ω	Circular frequency

ABSTRACT

This study of control-surface flutter was initiated because of serious hull vibration on destroyers of the DD 931 Class. The source of the vibration had been traced to the twin rudders by the Boston Naval Shipyard.

For making experimental observations on control-surface flutter phenomena in the towing basin, the David Taylor Model Basin constructed the TMB Control-Surface Flutter Apparatus. With this equipment, a marked decrease in overall damping was demonstrated when the downstream mass unbalance was increased during underway tests.

A condition in which hydrofoil oscillatory motion results in low damping without oscillatory instability is defined as "subcritical flutter." Such a condition, which greatly magnifies the sensitivity of the mechanical system to external sources of vibration, may be quite significant in the field of naval architecture. Analyses varying in complexity are explored and compared with experimental results.

INTRODUCTION

The control-surface flutter study at the David Taylor Model Basin was undertaken because of an unusual hull vibration condition observed during the preliminary acceptance trials of the USS FORREST SHERMAN (DD 931). The latter is discussed in considerable detail in Reference 1.* The mode of vibration in question was identified as a 3-node horizontal mode of the entire hull. The amplitude in this mode increased as the speed increased above 25 knots; the frequency, however, remained constant.

When the Boston Naval Shipyard[1] traced the source of this vibration to the twin rudders and corrected the condition by changing the original 3-degree toe-in** angle to a 1½-degree toe-out angle, the Bureau of Ships assigned to the Model Basin the task of explaining this phenomenon. An investigation of flow conditions at the rudders which might contribute to the vibration was made at the Model Basin.[2] As a result of a suggestion by the Model Basin that this vibration could be a flutter phenomenon, a specific project on control-surface flutter was authorized by the Bureau of Ships.[3] However, it was not assumed that the DD 931 problem had been identified as a flutter phenomenon.

Flutter problems, with the possible exception of the singing propeller,[4,5] have been extremely rare in naval architecture. The possibility of rudder flutter was pointed out by

---

*References are listed on page 42.

**To avoid conflict with Reference 1, toe-angle will be used to refer to the trailing edges of the rudders. Toe-in means toward the ship's centerline. Ordinarily, it would be preferable to use toe-angle as defined by Saunders;[14] i.e., with respect to the leading edges.

Wilson,[6] although he cited no specific case. However, the general impression has been that flutter phenomena are not likely to occur in the marine field.

This investigation is of a preliminary nature. The results are presented at this time because of the scarcity of experimental data and the lack of awareness that flutter phenomena, in the broad sense of the term, are possible in the field of naval architecture. The aim was not only to explore the basic phenomenon of control-surface flutter but also to expedite the development of an analytical method for predicting flutter speeds in the marine field. The experiments were initially planned on the assumption that critical flutter would be encountered. As the basis for the design of the apparatus, a simplified analysis was used involving gross assumptions as to the nature of the oscillatory hydrodynamic lift and moment. It was recognized that the analysis might be oversimplified, and that critical flutter might not be obtained. Therefore, the apparatus was designed for a maximum permissible speed considerably higher than the critical speed predicted by the simplified analysis. The location of the center of gravity (c.g.) and the zero speed damping could also be varied widely. Despite the versatility of the apparatus and the wide range of variables covered in the tests, critical flutter was not obtained; that is, no unstable or self-excited vibration was observed. However, a vibratory condition was obtained in which the overall damping had been severely reduced. This oscillation consisted of a very large magnification of a small excitation. Since this phenomenon is shown to be caused by the same mechanism which produces critical flutter, the definition of flutter has been extended herein for use in describing the observed phenomenon.

Inasmuch as the simplified analysis was shown to be overly conservative, computations were made on the basis of two slightly more complicated analyses. Nevertheless, the limited extent of this study does not permit an adequate evaluation of methods of flutter prediction as applied to naval architecture at this time.

A vast amount of material on flutter, both theoretical and experimental, has been published in the aeronautical field. The classical theory of flutter in an incompressible fluid, as treated in References 7, 8, 9, and 10, is transferable to the field of naval architecture provided that possible effects of cavitation can be neglected. In spite of the work available in the aeronautical field, it was considered necessary to conduct basic experiments on control-surface flutter in the marine field for the following reasons. If flutter should occur, the Strouhal numbers* are apt to be much higher in the marine field than in the aeronautical field, since the foil chords and frequencies of vibration are of the same order whereas the speeds of ships are about one-tenth those of aircraft. Even in the aircraft field, experiments have shown that the fluid dynamic forces which cause flutter depart from the theoretically predicted values at high Strouhal numbers.[8]

---

*The Strouhal number (also called the reduced frequency) is defined as the dimensionless ratio $\frac{\omega b}{S}$, where ω is the circular frequency of oscillation,

b is some characteristic body dimension, and

S is the speed of undisturbed fluid relative to the body.

In flutter work, the characteristic body dimension is taken to be the half-chord of the foil.

Another important factor is the difference in fluid densities which makes the dynamic pressures in the marine field greater than those in the aircraft field at operating speeds. For instance, the dynamic pressure in air at sea level at 400 mph is about 400 psf, and in water at 30 knots is about 2500 psf.

Viscosity effects may also differ considerably in the two fields (the viscosity of water being about 60 times as great as that of air). The Reynolds numbers* applicable to the experiments discussed in this report are of the same order of magnitude as those which apply in airfoil experiments; namely, 10^6. In the case of the DD 931 at high speeds, the Reynolds numbers applicable to the rudders are of the order of 10^7.

In view of the difference in construction and materials, the dependence of structural damping on amplitude and frequency might be expected to be different in the marine field from that in the aircraft field. Thus there were ample reasons for initiating a basic exploration of the control-surface flutter problem in the marine field.

BACKGROUND

The control surface, as used in naval architecture, is essentially a hydrofoil attached to a shaft passing into the hull through a bearing and packing gland. The principal examples of such devices are rudders, submarine diving planes, and activated fin stabilizers. It is obvious without detailed analysis that, if the center of mass (including added mass) of such a device is not on its shaft axis, an acceleration of the shaft in a direction normal to this axis and to the direction of flow results in a tendency to twist the shaft, and hence to change the angle of attack of the hydrofoil. A rudder assembly is flexible in bending, torsion, and shear, and it may have normal modes of vibration involving considerable torsion whose frequencies fall in the range of frequencies of horizontal flexural modes of the hull. In the latter modes, the rudder stock (being vertical) moves in a direction normal to the flow. If mass unbalance** of the rudder exists, a change in angle of attack is to be expected under horizontal acceleration. Thus, mass unbalance provides a coupling between the transverse and rotational motions, in addition to any other coupling that may be present. If the rudder natural frequency is near that of a horizontal mode of the hull, large rudder oscillations will occur under horizontal hull vibration.

The oscillatory stability of a system (control surface coupled with a hull mode) with two or more degrees of freedom will be considered. *Classical flutter* is a dynamically unstable, self-excited vibration of an oscillatory system immersed in a field of fluid flow. Since the

---

*The Reynolds number used here is based on chord length and is $\frac{2bS}{\nu}$ where $2b$ is the chord length,

S is the speed of the foil, and

ν is the kinematic viscosity of the fluid.

**Mass unbalance is used here interchangeably with the first moment of mass of the rotational portion of a foil system, and includes an allowance for added mass effect.

vibration is unstable, the net flow of energy to the system is positive; that is, the overall damping is negative. The dynamic stability of such a system depends upon its speed relative to the fluid. The lowest speed at which the system is neutrally stable is called the "critical flutter speed." At the critical speed, the net flow of energy to the system is zero and the overall damping is zero.

An important concept is that of neutral stability. Null damping and a balance of energy flow are equivalent terms. To obtain some quantitative measure of the stability of the system under investigation here, the experimental results are described in terms of damping and the analytical results in terms of the Routh discriminant (to be discussed later). The damping in a flutter mode can be referred to any degree of freedom since it vanishes simultaneously in all degrees of freedom.

The forces involved in a flutter phenomenon are both structural and fluid dynamic in origin. In linearized theory, they are proportional to acceleration, velocity, or displacement. The fluid dynamic forces are functions of the speed of the foil. Ordinarily, fluid dynamic forces exist which increase the damping with speed, thus tending to stabilize the system.

The essence of flutter action is that the oscillatory motions of the hydrofoil evoke fluid dynamic forces which are so phased and of such magnitude as to reduce the overall damping of the system. The term *overall damping* includes all effects contributing to the rate of decay or buildup of a free vibration. In order for flutter action to occur, the motions in the different degrees of freedom must have the proper phase and magnitude relative to one another. It can be shown that the coupling due to mass unbalance or fluid forces greatly influences the phase relation between the displacements in the various degrees of freedom.

The term "subcritical flutter" is introduced here to designate a condition in which the damping has been reduced (by the same mechanism which produces classical flutter) to such a small (but positive) value that the system becomes very sensitive to external sources of vibration. The resulting vibration is barely stable; hence a small, externally applied oscillatory force causes a very large response of the system. Hereafter, the term "flutter action" will be used to apply to subcritical conditions, since the mechanism is the same as that which produces classical critical flutter. The use of the word *flutter* in the terms flutter action and subcritical flutter, as applied here to conditions in which an oscillation is not unstable and not self-excited, is clearly an extension of the commonly accepted definition of flutter.

A graphical description of an actual aircraft condition which, in this report, would be designated subcritical flutter, is given in Reference 11 by Fraser, Duncan, and Collar. Figure 12.1.3 on page 358 of that reference shows the variation of damping with speed computed for an oscillatory system considered as having two degrees of freedom. The modes involved were an aircraft fuselage torsion mode and rotation of the rudder. It is similar to the case of DD 931 in that the torsional motion of the control-surface member is coupled with a mode of the main structure which involves horizontal displacement of the rudder axis.

TMB CONTROL-SURFACE FLUTTER APPARATUS

The TMB Control-Surface Flutter Apparatus, illustrated in Figure 1, was designed to basic specifications prepared at the David Taylor Model Basin, and was built at the Model Basin.

No attempt was made in the design to simulate an actual rudder-hull system. On the contrary, the aim was to produce an ideal system of two degrees of freedom, the physical constants of which could be experimentally determined and which could hence serve as a basis for checking flutter analyses based on various assumptions as to the nature of the oscillatory lift forces and moments.

The operational specifications were as follows:

1. Hydrofoil to be rectangular outline with 18-inch chord and 18-inch depth, the profile being the NACA 0015 section.

2. Hydrofoil to be located directly below a surface plate, the latter fixed to the towing carriage and the former free to oscillate torsionally about a vertical axis which could be located either at the forward quarter-chord position or the half-chord position while the supporting assembly could oscillate in translation in a horizontal direction normal to the direction of travel of the towing carriage.

3. Provision to be made for setting the hydrofoil at angles of attack of 0 degree, 2½ degrees right, or 5 degrees right when in rest position.

4. Natural frequencies in translation with rotation locked and in rotation with translation locked, both tunable to 4.0 cps.

5. Towing speeds permissible up to 20 knots.

6. Mass unbalance of rotatable element adjustable by means of sliding weights, permitting shifting center of mass either upstream or downstream.

7. Eddy current dampers to be provided for increasing the damping in either the translational or rotational degree of freedom.

8. Flutter speed predicted by formula (given on page 16) to be in lower half of permissible speed range.

The following additional features are noted. The preset angles of attack of 0 degree, 2½ degrees, and 5 degrees are nominal angles with no torque on the foil. The eddy current dampers provide a controllable damping which can be varied by changing the current through the windings in addition to the damping inherent in the apparatus. The uncoupled natural frequencies in translation and rotation were chosen to be the same as the frequency of the rudder-excited hull vibration encountered on DD 931. The apparatus was designed specifically for mounting on Towing Carriage No. 5, a high-speed carriage illustrated in Figure 20 of Reference 12. Although the 20-knot upper-speed limit was much below the maximum permissible carriage speed, it was sufficiently high to permit adequate experimental determination

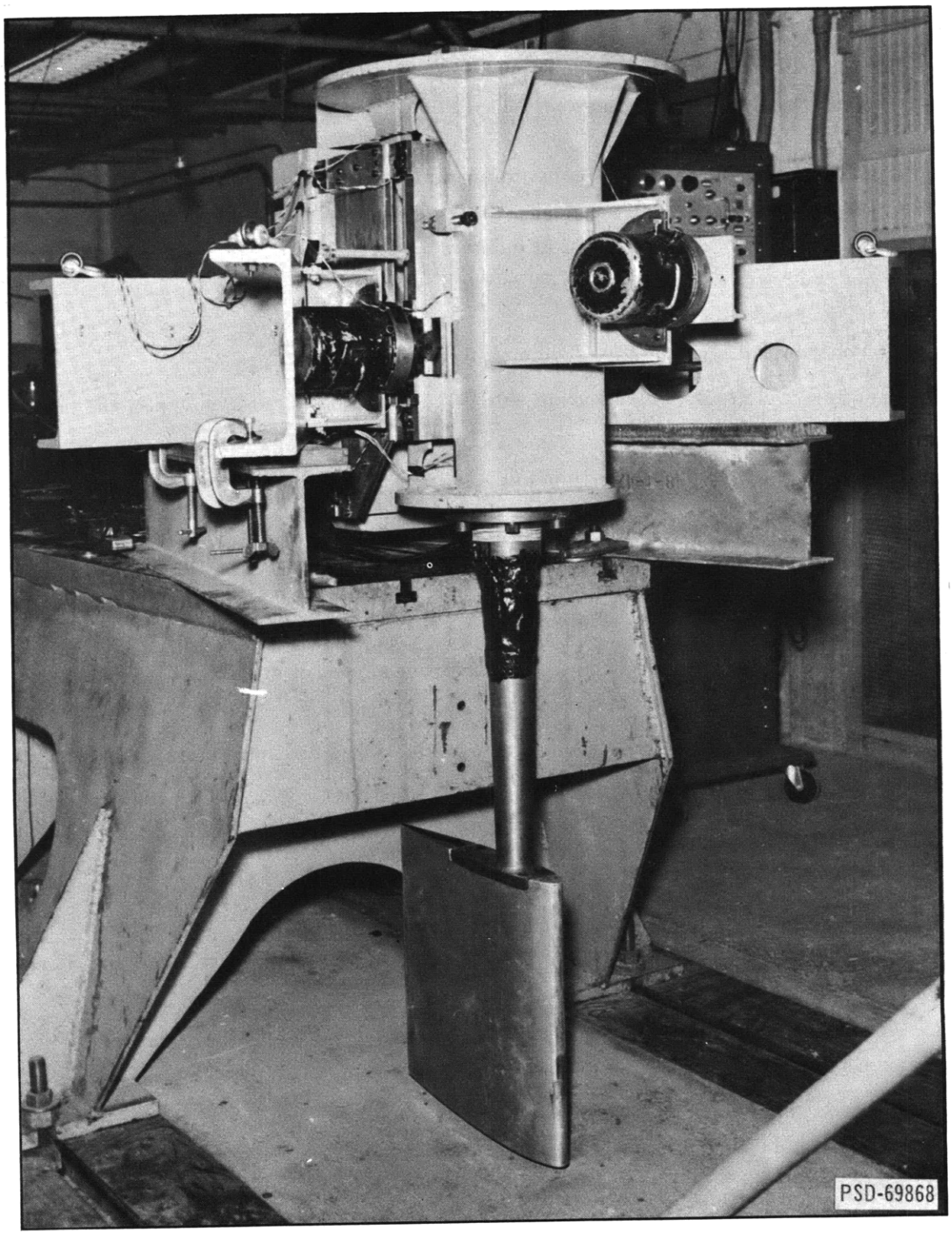

Figure 1 – TMB Control-Surface Flutter Apparatus

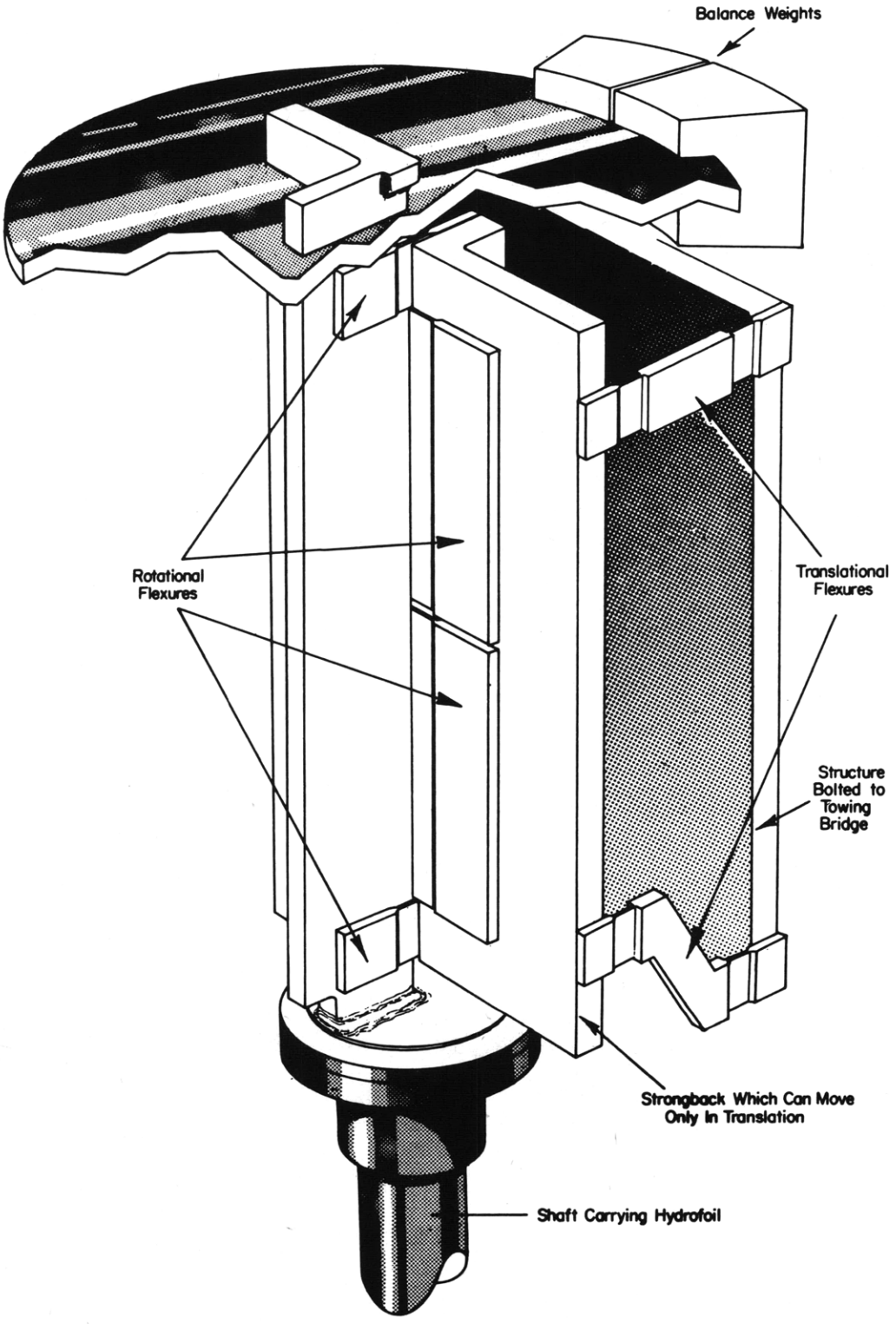

Figure 2 – Sectional Elevation of TMB Flutter Apparatus

of damping as a function of speed. The principal design calculations are summarized in Reference 13, which is proprietary to the David Taylor Model Basin.

Figure 2, which is a sectional elevation, shows the essential features of the design of the apparatus. A vertical shaft carries a standard NACA symmetrical hydrofoil, and is relatively rigid but attached to an assembly which can rotate with respect to a heavy strongback. The rotational assembly is connected to the strongback by means of a set of flexure springs, which in this case gives action identical to that of torsion springs. The stiffness of these springs and the mass moment of inertia determine the rotational natural frequency. The strongback, in turn, is suspended by flexures lying in a vertical plane from another heavy structure which is bolted directly to the towing bridge of the carriage when assembled for test. These latter flexures permit the foil, shaft, and strongback to translate horizontally. The stiffness of these flexures, together with the total mass which translates (including added mass), determines the natural frequency in translation. Thus this design constrains the foil to two degrees of freedom; horizontal translation perpendicular to the oncoming flow, and rotation about a vertical axis. Provision is made for locking each degree of freedom separately, and for limiting the amplitudes. As can be seen from Figure 3, when the apparatus was assembled on the towing bridge, the horizontal surface plate (which itself was completely submerged under test conditions) extended over the hydrofoil in order to minimize wave effects.

The mass unbalance can be varied by the use of sliding counterweights clamped along the periphery of the circular disk at the upper end of the rotatable assembly. Since the center of the disk coincides with the axis of rotation, the mass unbalance can be varied without changing either the mass or the mass moment of inertia as long as the same counterweights are used. Hence the natural frequencies in the separate degrees of freedom remain constant for all counterweight positions. The center of mass of the entire assembly can thus be shifted from a downstream position through the balanced position (on the axis) to an upstream position.

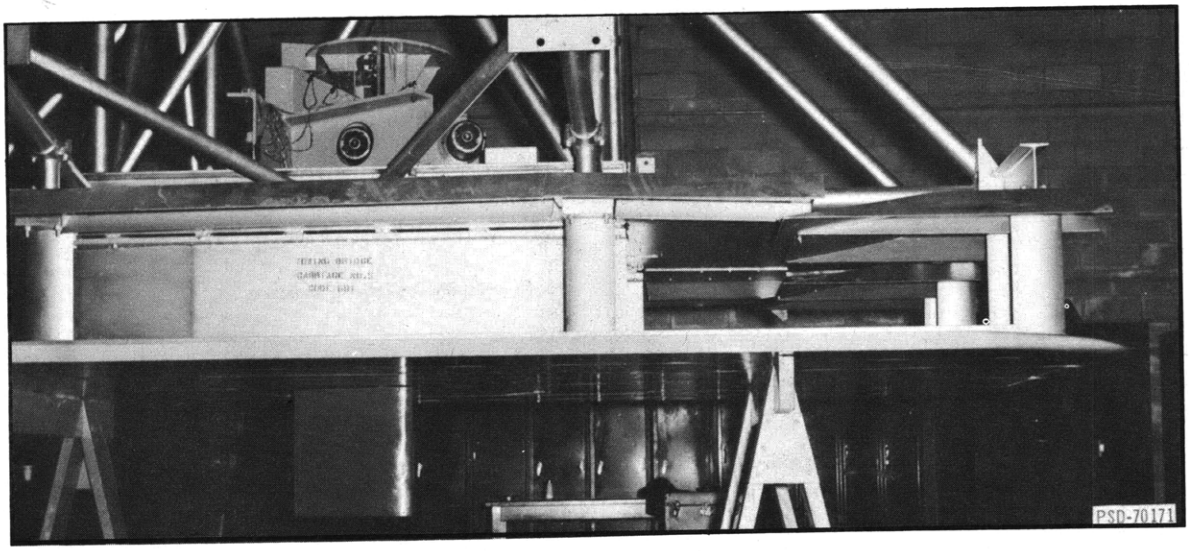

Figure 3 – TMB Flutter Apparatus Installed on Towing Bridge

The limiting values of mass unbalance are -0.9 and $+2.0$ lb-sec^2, respectively. It should be noted that this convenient arrangement for varying the mass unbalance is feasible only because in this design the shaft and hydrofoil are relatively rigid compared with the flexibility of the torsion springs. The balance thus attained is not a dynamic balance as the term is applied to continuously rotating bodies, since the axis of rotation is not a principal axis of inertia of the rotating assembly. It was not presupposed in determining the specifications for this apparatus that a similar balancing scheme would be feasible in an actual rudder installation.

Wire resistance strain gages were installed on both sets of springs, and the strain signals were fed to a Sanborn Recorder installed on the towing carriage. This gave both steady and alternating rotational and lateral deflections in the apparatus. Strain gages on the vertical shaft itself were intended only to verify stress levels and not to provide test data.

The constants of the TMB flutter apparatus, as determined experimentally, are given in Table 1.

TABLE 1

Constants of TMB Control-Surface Flutter Apparatus

Symbol	Definition	Numerical Value	Dimensions in Inch-Pound-Second System
A	Lift constant of the hydrofoil (lift force per unit angle of attack per unit velocity squared)	0.034	lb-sec^2/in.^{2}
C	Linearized damping constant for the translational degree of freedom at zero speed	0.375	lb-sec/in.
c	Linearized damping constant for the rotational degree of freedom at zero speed	22.3	in-lb-sec
h	Distance from the axis to the c.g. of the rotating assembly based on mass plus added mass (positive if c.g. is downstream)	variable; max. value 1.64	in.
I	Effective mass moment of inertia of the rotating assembly with respect to its axis including the added mass moment of inertia	62.3	in-lb-sec^2
K	Translational spring constant	867	lb/in.
k	Torsional spring constant	37,300	in-lb
M	Mass of the apparatus that moves only in translation	0.23	lb-sec^2/in.
m	Mass of the hydrofoil including the mass of the entire assembly that rotates with it and the added mass for translation	1.23	lb-sec^2/in.

EXPERIMENTAL PROCEDURE AND RESULTS

These experiments by no means exhausted the possibilities of the TMB flutter apparatus. They are presented at this time because it is believed that significant results have been obtained in a field in which there is a serious lack of experimental data.

DETERMINATION OF CONSTANTS

Before any test runs were made, all constants of the system that could be experimentally determined were so obtained. These values are given in Table 1. It was particularly important to calibrate the strain-recording system in terms of both rotational and translational displacements of the hydrofoil. It was also important to determine the inherent damping of the system, the mass unbalance for given settings of the counterweights, and the natural frequencies of the system in rotation and translation with the carriage at rest.

The spring constants K and k were obtained as the ratio of a static force or moment to the corresponding displacement in each degree of freedom separately. The natural frequencies were obtained in air and in water for the separate degrees of freedom by reading the recorded natural vibrations following an initial deflection at zero speed. The total mass $(M + m)$, including added mass, which vibrates in translation was obtained as the ratio of the translational spring constant to the square of the natural frequency in water. The total mass in air was also obtained as the ratio of the translational spring constant to the square of the natural translational frequency in air. The total translational mass in air was checked by weighing, and less than 4-percent difference was found between the two values. The difference between the translational masses in air and in water gave the added mass in translation. The mass m was obtained by weighing the rotational portion of the apparatus and combining its mass with the added mass in translation. The mass M of that portion of the apparatus which translates but does not rotate was obtained by subtracting m from $M + m$. Since that part of the apparatus which can move only in translation is entirely out of water, no added mass is involved.

The moment of inertia I was obtained as the ratio of the rotational spring constant to the square of the natural frequency in rotation *in water*. Thus this value includes the moment of inertia due to added mass at zero speed. This value agreed with the computed design value.

To check the values obtained for the mass $(M + m)$ and the mass moment of inertia I, the counterweights were removed, thus changing the mass and the mass moment of inertia by accurately known amounts. The natural frequencies were then measured and were found to agree with the frequencies predicted on the basis of the changed inertias.

The first moment of mass or mass unbalance (mh), including the moment due to added mass, was obtained by the following method. The position of the counterweights was varied until no discernible beating occurred between the two degrees of freedom when both were excited with the foil in water at zero speed. It was assumed that this null beating condition was obtained when the c.g. of the apparatus (including added mass and counterweight masses)

coincided with the axis of rotation, $h = 0$. Thus the mass unbalance mh was obtained for any position of the counterweights simply by multiplying the mass of the two counterweights by the downstream displacement of their common c.g. from the null position. It was assumed that added mass effects are independent of speed.

The damping constants C and c were obtained for each degree of freedom with the other locked, by measuring the rate of decay of free vibrations in water. These constants were slightly dependent on the amplitude. The values given are averages corresponding to the observed amplitudes.

The lift coefficient of the foil was obtained by measuring the force on the foil at various speeds and attack angles with the rotational degree of freedom locked.

In the tests in still water, the natural frequencies of the translational system with the rotational locked and of the rotational system with the translational locked were both tuned close to 4.0 cps. The computations made, up to this writing, were based on the values of the parameters applicable to this test condition. It was predicted analytically and verified experimentally that for this condition the two natural frequencies of the combined system in still water were 3.7 cps (out-of-phase mode) and 4.5 cps (in-phase mode). The coordinate system applied in this case gives phase relations which are the reverse of those found in the ordinary rectilinear system of two degrees of freedom.

OBSERVATION OF STEADY HYDRODYNAMIC MOMENT

An important observation made in the initial runs for calibrating the apparatus was that the hydrofoil was not hydrodynamically balanced; that is, the line of action of the steady lift force did not pass through the axis of rotation. Such balance had been assumed in the design for the condition in which the axis was positioned at the forward quarter-chord point. As pointed out in subsequent sections, the observation of hydrodynamic unbalance was important in the attempt to correlate experimental results with analytical predictions. Although the hydrofoil was set for a nominal zero angle of attack for certain runs, it was found on all runs that steady components of both lift force and moment developed, once the carriage got under way. It was also found that the center of steady lift was actually forward of the quarter-chord position or axis location for all settings of angle of attack. The distance L of the center of lift forward of the axis varied with the zero speed attack angle α_0 and was observed to be practically independent of speed. The three values of L derived from the steady lift and moment measurements are shown in Table 2, together with the distance from the leading edge of the foil as a percentage of chord length $\left(100\,\frac{(b/2)-L}{2b}\right)$. Thus the length of the hydrodynamic moment arm is considerable at small attack angles, and indications are that it is a nonlinear function of attack angle. Such a condition produces a negative torsion spring effect which increases with speed. At a high enough speed, this would lead to the torsional divergence condition.

TABLE 2

Location of Center of Steady Lift

α_0 Nominal	L inches	$\frac{(b/2)-L}{2b}$ percent
0	2.8	9.4
2.5	0.6	21.7
5	0.6	21.7

CARRIAGE VIBRATION

The experimental procedure was complicated by vibration of the towing carriage itself. However, extraneous sources of vibration would be encountered in any facility available for experiments of this nature, and no attempt was made to utilize a different test facility. Although methods were devised for taking account of the carriage vibration, they are not discussed in this report.

Measurements on the towing carriage revealed that it vibrated in two modes whose natural frequencies fell in the range of frequencies observed in the records obtained from the flutter apparatus. The first of these was the heaving mode with a natural frequency of 4.5 cps, and the second was the transverse rocking or rolling mode with a natural frequency of 6.0 cps. There was no reason to expect a coupling of the heaving motion of the carriage with vibration in the apparatus, and it was found that such coupling was negligible. Special tests were conducted with the carriage at rest, to determine how the natural modes of the carriage affected the apparatus. When the carriage was excited by impact in its heaving mode, negligible apparatus response ensued. Only the rolling mode affected the apparatus measurably. When the towing carriage was under way and the frequency recorded from the apparatus was 4.5 cps, the carriage, in addition to heaving, was executing a forced rolling at the same frequency. A study was then made to determine the source of carriage excitation when under way. It was found that transient vibrations of the carriage were excited by acceleration and deceleration as well as by slight track irregularities. The drive motors which are connected to worm wheels engaging gears on the drive-wheel shafts rotate at 0.9 rps per knot carriage speed. These motors are a conceivable source of carriage vibration. However, it was observed that when all frequencies picked up by the apparatus during steady-speed runs were plotted on a basis of carriage speed, the points concentrated along lines radiating from the origin. The slopes of these lines were found to be integral multiples of the slope of the line giving the drive-wheel frequency on a basis of carriage speed. This plot is shown as Figure 4, where the frequency f is given in cps. The excitation was apparently due to the slight out-of-roundness of the drive-wheel surfaces. The drive wheels have rubber tires filled with water.

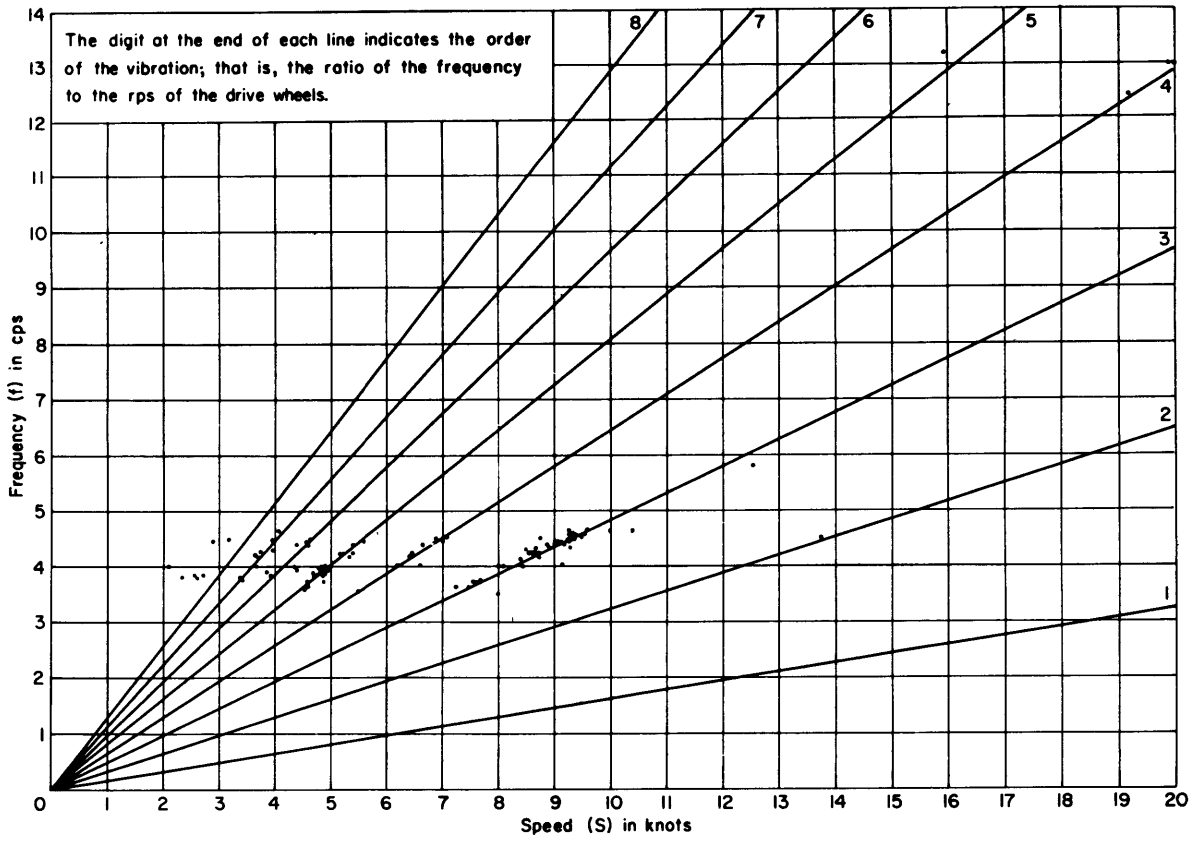

Figure 4 – Correlation between Recorded Frequencies and Drive-Wheel Harmonics

At a towing speed of about 9.3 knots, the amplitudes of carriage vibration, as measured directly, were as follows:

Heaving: 13 mils double amplitude at 4.5 cps;

Rolling: 1.2×10^{-5} radians double amplitude at 4.5 cps (nonresonant);

Rolling: 1.4×10^{-4} radians double amplitude at 6.0 cps (resonant).

On certain runs, signals from vibration pickups that were attached directly to the structure supporting the flutter apparatus were recorded directly on the oscillograms, giving the strain signals from the apparatus. Although these indicated the horizontal vibration to be predominantly of a frequency of 6.0 cps, the signal that could be obtained with this recording system was too small for quantitative measurement. Horizontal vibration at the carriage walkway level was below the sensitivity (0.5 mils double amplitude (d.a.)) of a TMB two-component pallograph at 9.3 knots. It is clear that under such circumstances caution must be used in analyzing the test data. It was obviously necessary to adopt a somewhat arbitrary background or "noise" level of recorded amplitude of the translational motion of the apparatus below which the vibrations recorded would not be considered significant. This level was taken as 20 mils d.a.

TEST RUNS

One of the objectives in the experiments was to determine the overall damping of the apparatus as a function of speed. Two quite independent methods of determining the damping of mechanical systems are in common use. One is to observe the resonance magnification of forced vibrations, and the other is to observe the rate of decay of free vibrations. Therefore, aside from the calibrations, two principal series of test runs were made:

Series A. Runs at different speeds with various settings of the mass unbalance and the nominal angle of attack, during which there was no external stimulus aside from the normal carriage vibration. The translational and rotational displacements were recorded on the oscillograph.

Series B. Impact tests in which the apparatus was excited by striking with a heavy timber while the towing carriage was under way, building up speed at a very slow rate (not exceeding 0.15 knot/sec), and the subsequent vibrations were recorded.

In all of these tests the elastic axis (axis of rotation) coincided with the forward quarter-chord position of the hydrofoil. The eddy current dampers were not used.

A tabulation of the test data is given in Appendix A. Examination of Series A data shows that the largest apparatus response (70 mils d.a.) was obtained at 9.3 knots for mh = 2.0 lb-sec^2. Figure 4 indicates that the third drive-wheel harmonic evoked this response. The rolling double amplitude of the carriage at the recorded frequency, however, was only 1.2×10^{-5} radians, as measured. Figure 5 shows plots of damping ratios DR on a basis of towing-carriage speed, with mass unbalance mh as a parameter as derived from the Series B tests. In the cases of low mass unbalance, the decay rate in the translational degree of freedom only was measured. A value of unity for DR indicates critical damping. The steady-run data suggest the possibility that the damping at 9.3 knots and mh = 2.0 lb-sec^2 was reduced to a value less than was obtained from the Series B tests at any speed.

In view of the known excitation from the carriage, the Series B data shown in Figure 5 were examined for possible correlation of low damping values and presence of carriage-wheel harmonics. In a number of cases, the impact occurred at a speed at which a drive-wheel harmonic frequency was close to the apparatus frequency. However, at many points this was was not the case so the large differences in overall damping ratios for different mass unbalance settings could not have been caused by carriage vibration. It was indicated that the low values at about 5.5 knots, 7.6 knots, and 9.6 knots for mh = 2.0 lb-sec^2 were influenced by carriage drive-wheel harmonics. However, this meant simply that if the carriage vibration had not been present a smoother plot would have been obtained.

A check on the possibility of cavitation indicated that it would not occur below 22 knots for the largest permissible angle of attack (5 degrees). See Reference 2.

A check of vortex shedding frequencies gave a value of about 400 cps at 9 knots for this hydrofoil at the relevant Reynolds number. See Reference 14.

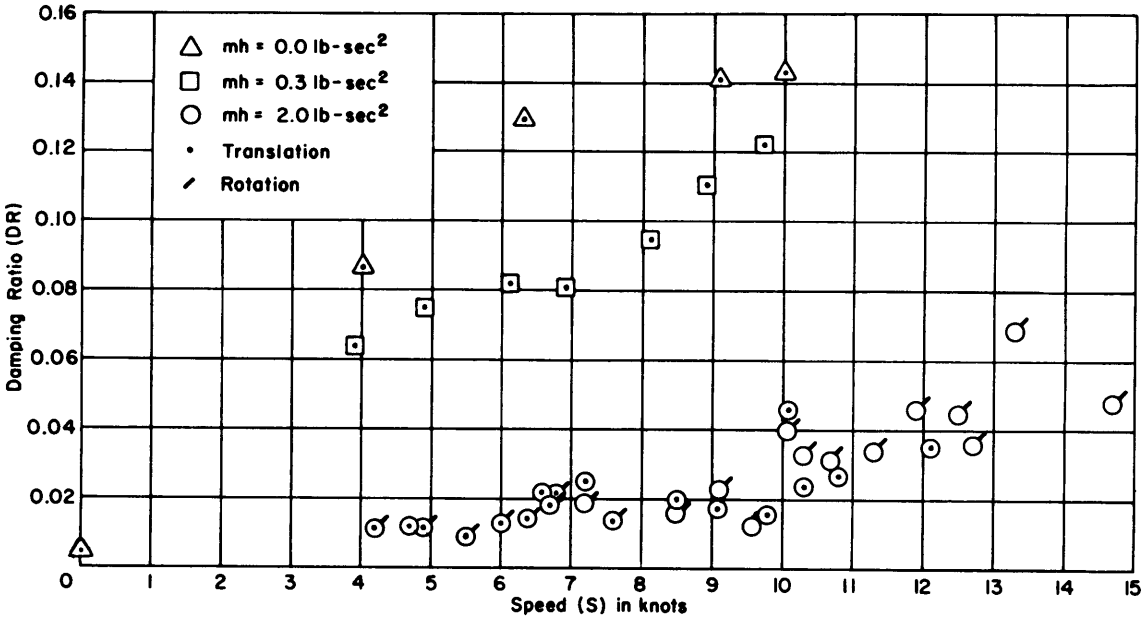

Figure 5 – Damping Ratios Derived from Impact Tests

ANALYTICAL PREDICTIONS

In deriving the dynamical equations, it was assumed that the structure supporting the translational flexures (*K* in Figure 8) had no motion in the direction of translation. Since there actually was carriage vibration in that direction, it is necessary to consider whether this could invalidate the analyses used.

The amplitudes recorded in the steady runs were definitely affected by the carriage vibration. This produced an effect similar to that caused by a vibration generator in aircraft flutter testing in flight. Such vibration, if appreciable, would require a modification of the analyses, since the values of displacement recorded would not indicate the true displacements normal to the flow direction. It was not considered necessary to modify the analyses because the carriage vibration amplitude in this direction was less than 0.5 mils d.a., whereas the adopted noise nevel was 20 mils d.a., and the recorded amplitude from impact tests was above 35 mils d.a.

SIMPLIFIED ANALYSIS

The design of the TMB flutter apparatus was based on a simplified analysis involving the assumptions:

1. that the two degrees of freedom were tuned to exactly the same natural frequency;
2. that the hydrodynamic moment due to circulation was zero (hydrodynamic balance); and

3. that the oscillatory lift force followed the steady lift force versus angle-of-attack relation.

It is generally recognized that in such a system flutter requires relatively close tuning of the separate degrees of freedom. This analysis is discussed in Appendix B. It yielded the direct formula for the critical flutter speed:

$$S = \frac{c}{2mh} + \sqrt{\frac{c^2}{4m^2h^2} + \frac{c}{Amh}\left[C + \frac{m^2h^2\omega^2}{c}\right]}$$

where S is the flutter speed. This formula predicted that the system would be stable up to a critical speed of 9.5 knots and unstable for all greater speeds for $mh = 2.0$ lb-sec^2.

EXTENDED SIMPLIFIED ANALYSIS

As shown in Appendix C, the introduction of a term for hydrodynamic moment due to circulation, by the expedient of assigning an appropriate value to the distance from the axis of the hydrofoil to the center of lift, yields the following pair of simultaneous linear differential equations:

$$I\ddot{\theta} + c\dot{\theta} + (k - ALS^2)\,\theta - mh\ddot{Y} + ALS\dot{Y} = 0$$

$$-mh\ddot{\theta} - AS^2\theta + (M + m)\,\ddot{Y} + (C + AS)\,\dot{Y} + KY = 0$$

where Y is the displacement of the axis of the hydrofoil in translation,

θ is the angular displacement of the hydrofoil, and

L is the distance from the axis to the center of lift (positive if center of lift is upstream).

The other symbols were defined previously.

These simultaneous equations can be solved by means of an analog computer such as REAC, or, if they are converted to algebraic form by the assumption of harmonic solutions, the determinant of the coefficients of θ and Y yields a frequency equation. This equation is a quartic in the complex frequency and in this case has real coefficients. Various ways of finding the roots of complex polynomials are discussed in Reference 7. However, the particular method used herein is discussed in Appendix C. The speed, frequency, amplitude ratio, and phase angle between the two degrees of freedom at the critical flutter condition and the value of the Routh discriminant at any speed could be calculated by the method used. Since the value of the Routh discriminant becomes zero at the speed of neutral stability, its numerical value is taken as a measure of the stability of the system. This point will be discussed further later. A method by which the exponential decay rate can be computed by use of the Routh discriminant is given in Reference 15.

MODIFIED THEODORSEN ANALYSIS

In the equations so far discussed, the alternating lift force due to the varying angle of attack has been treated as though the variation were at such a slow rate that the relation between the steady lift force and the steady angle of attack applied. This assumption was also applied to the corresponding moment. These assumptions effect greater simplifications than the quasi-steady assumptions used by aerodynamicists, and discussed in References 7, 8, and 9. By use of these assumptions, certain lift and moment terms which occur in the quasi-steady expressions are omitted. Those terms which are omitted would be written in this notation as a lift force $3/2\ Ab\dot{S\theta}$ and as a moment $-1/2\ Ab^2\dot{S\theta}$. Since these terms are proportional to the angular velocity, this lift force provides additional coupling between the degrees of freedom, and the moment term provides additional angular damping.

Theodorsen[10] and others have considered the problem of the forces and moments acting on oscillating airfoils using potential flow theory. Those studies arose in connection with the problem of flutter of aircraft wings, and the treatment included consideration of the angular deflection of an aileron relative to the wing. Theodorsen considered the idealized problem of a thin, rigid hydrofoil of infinite aspect ratio in a field of two-dimensional flow in the absence of structural damping. However, it is helpful to consider the TMB flutter apparatus as a special case of the problem considered by Theodorsen with the aileron locked at zero angular displacement relative to the wing. Modifications of Theodorsen's lift-force and moment expressions were made for application to the TMB flutter apparatus. The first modification is similar to the quasi-steady assumption sometimes made when the reduced frequency is small. In the quasi-steady assumption, Theodorsen's function is replaced by unity.[8] In the case of the TMB apparatus, the reduced frequency is relatively high, however, and Theodorsen's function is assumed to be equal to one-half. The second modification made was to include a hydrodynamic moment due to circulation. This analysis is described in Appendix C. Since the above modifications yield real coefficients in the equations of motion, the method of calculation used was the same as in the extension of the simplified analysis. It can be shown that the simplified analysis can be established as a special case of Theodorsen's analysis.

COMPARISON BETWEEN EXPERIMENTAL RESULTS AND ANALYTICAL STUDIES

In comparing the experimental results with analyses, it is essential to keep in mind two important aspects of the situation. The first of these is that flutter action, in the sense of the extended definition given in this report, can take place without causing unstable oscillations. When this happens, the reduction in overall damping may be sufficient to cause vibrations that are severe, from the naval architect's point of view, even though the absolute amplitudes may be far below those encountered in aircraft flutter. The other aspect is that the tuning of the rotational degree of freedom can be greatly affected by hydrodynamic

unbalance. This point is emphasized in Reference 6.

First the critical speeds will be considered. As was previously stated, no unstable or self-excited vibrations were observed. Thus the only analyses which can be said to agree with experiment are those which yield no critical speeds over the range of speeds and mass unbalance covered in the tests. The calculated critical speeds are shown for wide ranges of values of mh and L in Figure 6. It is to be recalled that the critical speeds are those at which the overall damping is zero. The critical speeds predicted from the simplified analysis are shown in Figure 6a as the curve marked $L = 0$. Since the frequencies in the two degrees of freedom are nearly in tune, the critical speeds predicted by means of the extended simplified analysis for $L = 0$ coincide with the values given by the formula on page 16.

The predicted critical speed curve and critical frequency for the value $L = 0.6$ in. are almost identical with those obtained for $L = 0$ and therefore are not shown. The curves marked $L = 2.8$, 6.41, 8.9, and 10.0 in. in Figure 6a are other predictions based on the extended simplified analysis. The critical frequencies are tabulated in Appendix C. The addition of the hydrodynamic moment due to circulation results in stabilization of the system at some speed higher than the lowest critical speed. Apparently, this stabilization is due to the detuning effect of this hydrodynamic moment. For L sufficiently large ($L = 10.0$ in.), the lowest critical speed is reduced considerably. No critical speeds were indicated by the extended simplified analysis below 20 knots and below $mh = 2.0$ lb-sec^2 for L between 6.5 and 8.5 in. In this respect, this analysis agrees with the experimental observations.

Calculations based on both the extended simplified analysis and the modified Theodorsen analysis were made for values of L up to $L = 10.0$ in., to establish the trend for large values and because high values of this effective moment have been observed. That is, the apparent center of lift can be forward of the leading edge of the foil.[16]

The computations based on the modified Theodorsen analysis indicated somewhat higher critical speeds. These occurred in a smaller range of large values of mh. No critical speeds were indicated below 20 knots and below $mh = 2.0$ lb-sec^2 for L between 8.1 and 10.0 in. Thus this modified Theodorsen analysis also agrees with the experimental observations, as far as critical speeds are concerned. (The critical frequencies predicted with the use of this analysis are shown in Table 6, Appendix C.)

The computed variation of the Routh discriminant with speed is compared with the experimental damping variation, since both are indicative of the stability of the system. Inasmuch as the lowest apparatus damping was observed for $mh = 2.0$ lb-sec^2, the discriminant variations with speed are shown for that case. It seems obvious that the numerical values of the discriminant $D(S)$ alone have little significance, and that they must be compared with some reference value. The most obvious reference value is the value of the discriminant at zero speed $D(0)$. Therefore the ratios $D(S)/D(0)$ were computed and used to indicate the variation of stability with speed. Curves of Routh discriminant ratios are shown in Figure 7. These are to be compared with the damping ratios shown in Figure 5.

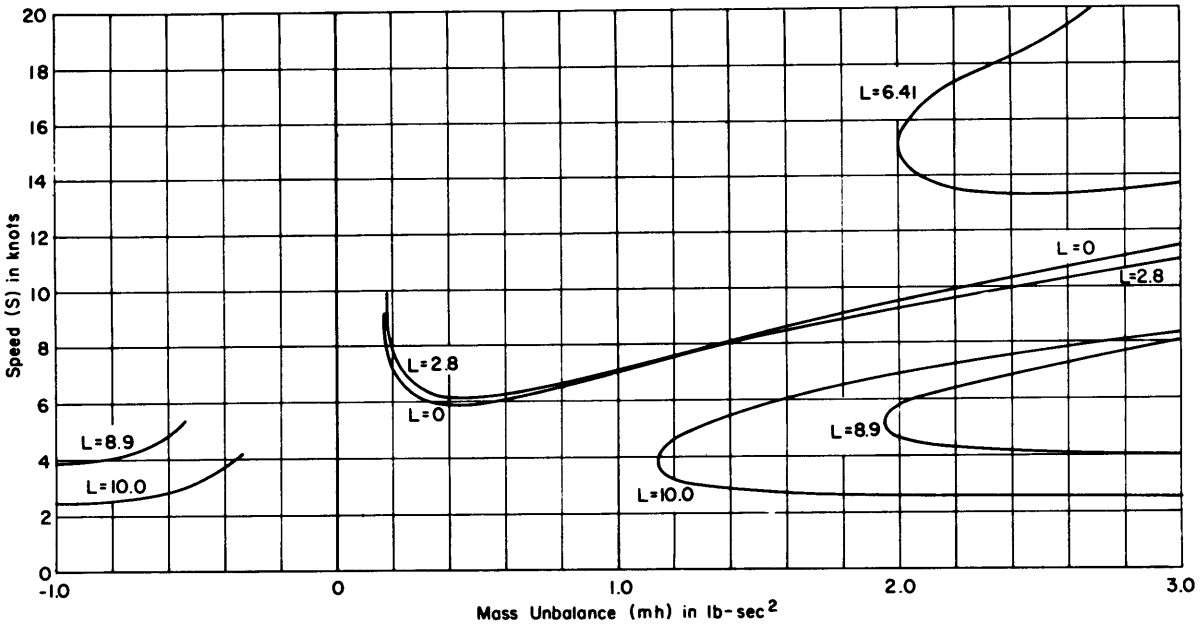

Figure 6a — Based on Extended Simplified Analysis

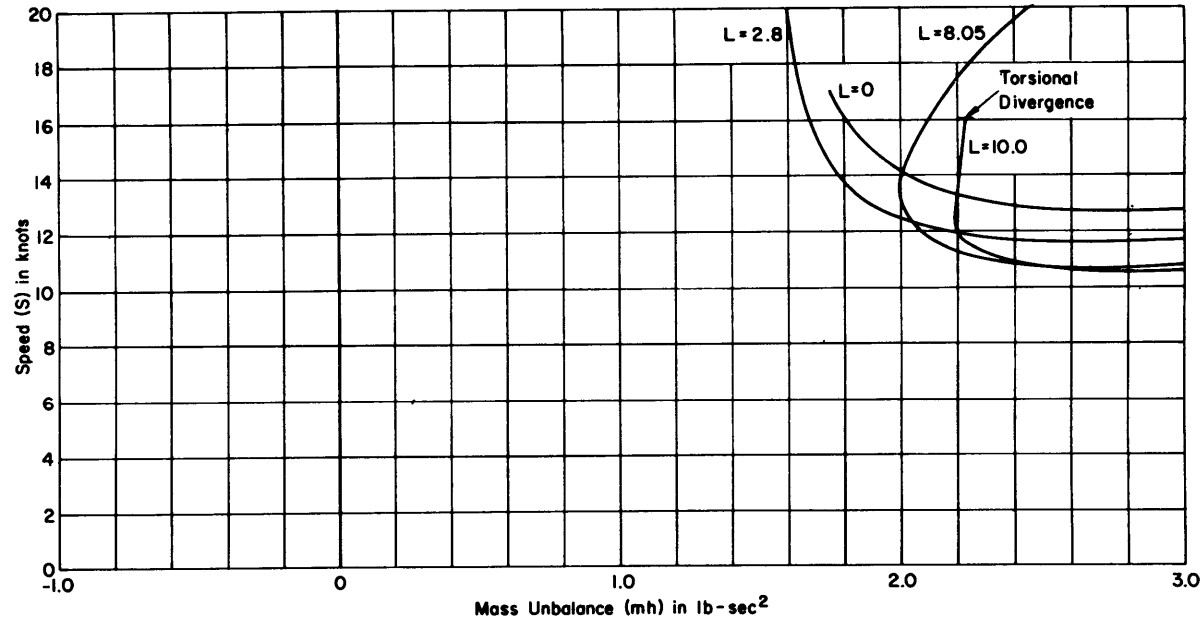

Figure 6b — Based on Modified Theodorsen Analysis

Figure 6 — Computed Critical Flutter Speeds

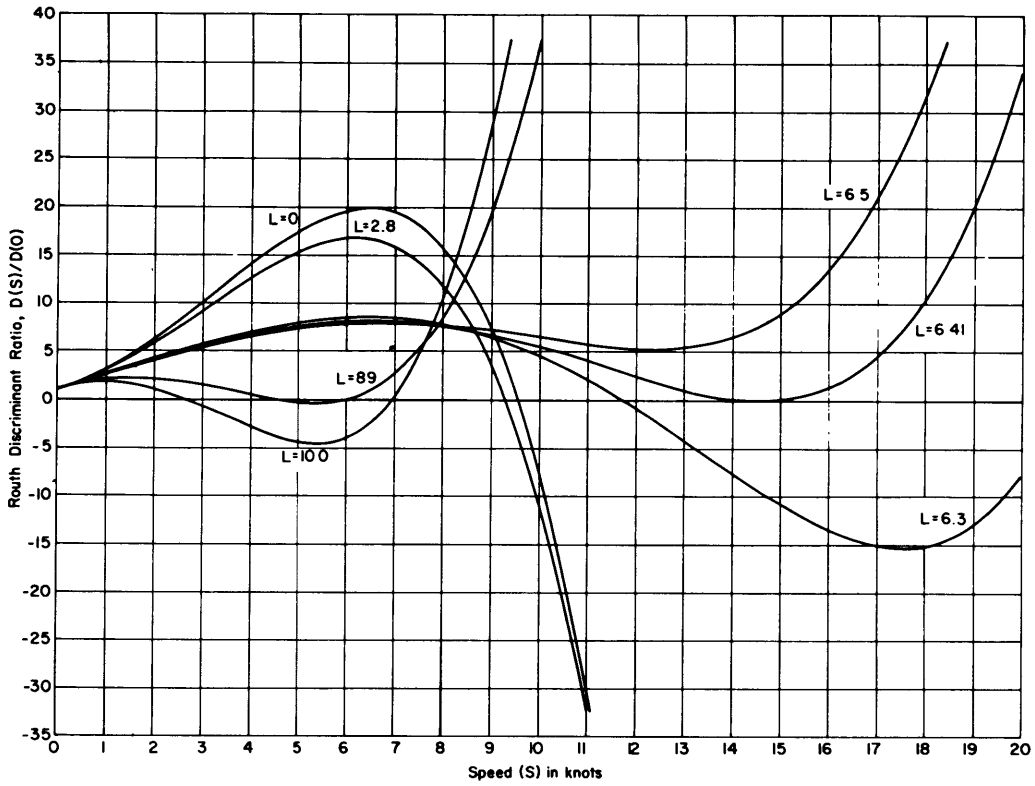

Figure 7a — Based on Extended Simplified Analysis

These calculations show that the stability of such a system can vary drastically for relatively small changes in the values of the parameters mh and L. This clearly indicates the possibility of a combination of parameters that will yield only a condition of subcritical flutter. It can be seen that the experimentally determined damping variation of the apparatus for mh = 2.0 lb-sec^2 and nominal zero preset angle of attack has the same trend as the discriminant ratio variation given by the analyses where larger values of L than those given in Table 2 were used. The discriminant ratio curve for L = 6.5 in. in Figure 7a and the curve for L = 10.0 in. in Figure 7b most nearly correspond to the experimentally determined variation of damping with speed.

The influence of preset attack angle on the amplitude of vibration in steady runs is indicated by the variation of the amplitude in translation with attack angle for a fixed value of the mass unbalance, as shown in Appendix A. For instance, for mh = 2.0 lb-sec^2, the maximum amplitude ($2Y_0$) is:

0.070 in. for α_0 = 0 at 9.33 knots

0.031 in. for α_0 = 2½ deg at 9.1 knots

0.020 in. for α_0 = 5 deg at 9.0 knots

In all these runs, the range of speed from 9.0 to 9.5 knots was covered.

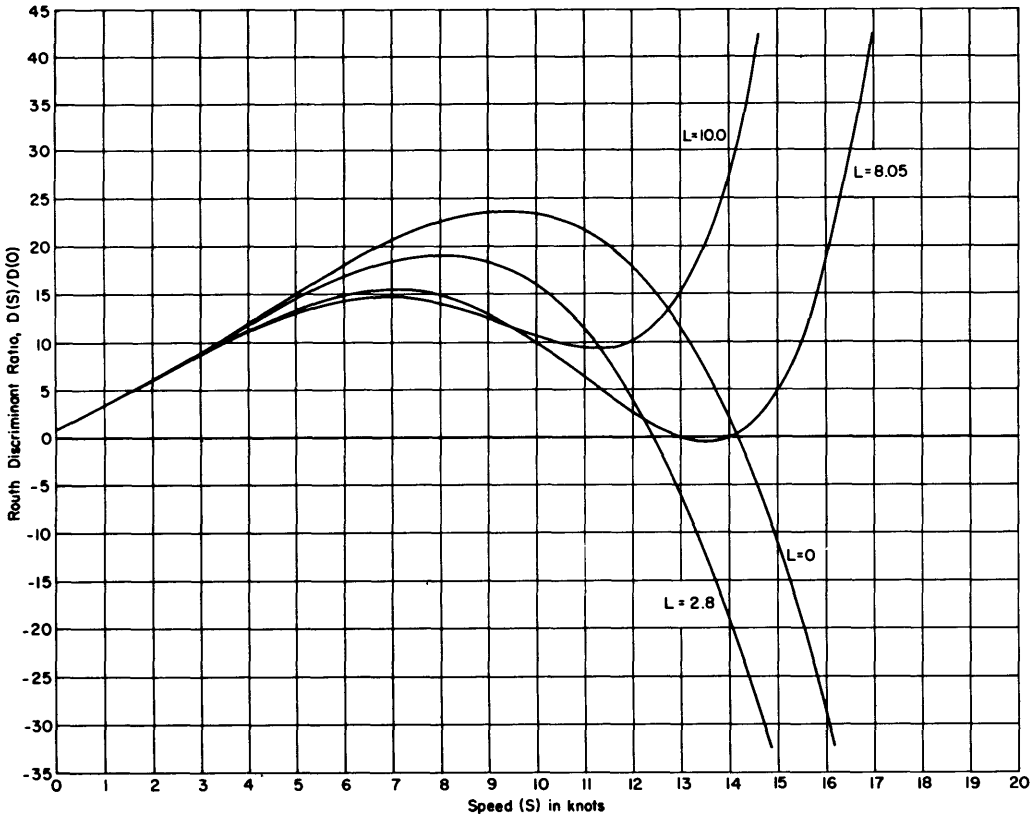

Figure 7b – Based on Modified Theodorsen Analysis

Figure 7 – Routh Discriminant Ratios

All curves are for $mh = 2.0$ lb-sec^2.

DISCUSSION OF RESULTS

The striking reduction in damping produced in the TMB flutter apparatus by increasing the mass unbalance, illustrated in Figure 5, can only be explained as due to subcritical flutter action. In these experiments, the harmonics of the drive-wheel frequency fell near the apparatus frequency in the speed range in which the damping was reduced by subcritical flutter action. This, rather than a high level of carriage vibration, accounted for the consistently large amplitudes measured in the apparatus at a speed of 9.3 knots for $mh = 2.0$ lb-sec^2. It would naturally be supposed that such a subcritical condition would develop into a critical condition as the speed was further increased, but the analysis shows why this is not always the case. A detuning action on the torsional degree of freedom due to hydrodynamic unbalance can cause the overall damping to rise again beyond a certain speed, thus preventing a true critical flutter condition.

The carriage vibration was helpful in revealing the subcritical condition after assurance had been obtained that the amplitude of carriage vibration was very low.

It is clear that a more painstaking analysis is necessary to definitely forecast a subcritical flutter condition than to estimate a critical flutter speed.

Although the critical flutter predicted by the simple formula was not obtained, the subcritical condition demonstrated could well be more significant in the field of naval architecture than could a critical condition. It is true enough that subcritical flutter is not a self-sustaining phenomenon, but a ship under way is subject to numerous sources of excitation, so that if there is a marked reduction in damping in a certain mode of the system this mode will probably be excited.

Although the naval architect has heretofore considered that flutter speeds were outside the range of ship operating speeds, there was at least a feeling that flutter could occur if ship speeds should ever be sufficiently increased. The phenomenon of subcritical flutter, however, was not generally recognized in the aircraft field, and an analysis that explores only for critical flutter would give little or no indication of such a possibility.

The data presented on page 20 show that the amplitude produced in a sub-critical flutter condition in such a system depends on the preset angle of attack.

RECOMMENDED METHOD OF CONTROL-SURFACE FLUTTER ANALYSIS

The aim in building the flutter apparatus and conducting the control-surface flutter experiments was not only to explore the basic phenomenon of control-surface flutter but also to expedite the development of an analytical method for predicting flutter speeds. It now appears, however, that methods of predicting subcritical flutter speeds warrant serious consideration in the field of naval architecture. Obviously, the ship designer desires the simplest analysis that will yield predictions consistent with experimental observations. The simplified analysis based on the assumption of hydrodynamic balance at all speeds does not agree with the experimental results. However, it was shown to be conservative and, moreover, yielded a direct formula for the flutter speed. It predicts a flutter speed for perfect tuning but, in general, the two degrees of freedom are not in tune and the critical flutter speed is likely to be higher. It requires, of course, that all the constants of the system be previously determined. The estimates should be made for a series of reasonable variations of the parameters A, mh, C, and c. If neither critical nor subcritical conditions are found for speeds up to 50 percent above the maximum operating speed, it is believed that a more extensive analysis is not necessary.

Clearly, a shipboard installation is vastly more complicated than this apparatus, but it is shown in Reference 17 that in any one of its normal modes a hull may be approximated by an equivalent system of one degree of freedom. Since the apparatus has more or less ideal characteristics, caution must be used in drawing conclusions as to what predictions can be made in actual shipboard installations by this method. However, it is recommended that, as a first step in exploring the possibility of a flutter condition involving the interaction

between a control-surface member and a hull, the control-surface member be reduced to an equivalent rigid-body torsional system.

The torsional stiffness of the shaft system must then be evaluated, and this, of course, may require considerable judgment as to the degree of fixity at the upper end of the shaft. The next most important consideration is the determination of the mass unbalance, and this must be based on a computation which includes an allowance for added mass. According to the simplified analysis, a flutter condition is to be anticipated only if the center of mass falls downstream. If this is the case, the torsional frequency should then be estimated by the elementary formula

$$\omega = \sqrt{\frac{k}{I}}$$

If this frequency falls in the range of the significant hull modes involving displacement normal to the axis of the control-surface member, then an estimate must be made of the frequency of the nearest mode. The entire hull is then reduced to an effective mass, spring, and dashpot for this mode by the method discussed in Reference 17. This then yields a lumped system of the type that can be treated by the equations applicable to the TMB apparatus.

What is most important is to be able to predict a lower limit for the overall damping of the system in the range of speeds in which the torsional oscillations of the control surface could be in tune with a flexural mode of the hull. This can be done by plotting as a function of speed the four terms appearing in the coefficient of $\dot{Y}$ in the equation on page 33, Appendix B. A standard of comparison then could be the value of C which represents the damping which the hull would have in the mode in question in still water with the rudder locked. It would be the value determined by a vibration generator test in still water in which the rudders are well out of tune with the hull.

Clearly, any assignment of a value to the overall damping of the coupled system below which the condition would be considered one of subcritical flutter is quite arbitrary. Although Figure 5 shows a striking reduction in overall damping between the balanced and maximum unbalanced conditions of the TMB apparatus, it does not show speeds at which the damping dropped below the zero-speed damping. The analyses shown in Figure 7 and in Figure 12.1.3 of Reference 11, however, clearly indicate such a possibility without ever reaching a condition of actual oscillatory instability. In practice, of course, the criterion would be whether the vibration resulting from the condition combined with external sources of disturbance produced "intolerable" levels of vibration.

The next question to consider is whether the control-surface member in its mean position is to operate at a small or a substantial angle of attack. If this angle of attack is substantial and the member is a hydrodynamically balanced hydrofoil, then the formula derived from the simplified analysis will yield a direct estimate of the flutter speed. If this speed is well above the highest operating speed, flutter is not to be anticipated, since the

assumption of coincidence of the torsional frequency with a frequency of the hull generally lowers the predicted flutter speed. If the flutter speed thus calculated falls in or near the operating speed range, a second estimate should be made by means of the more advanced methods given in Appendix C, with no assumption as to coincidence of the natural frequencies.

The assumption of hydrodynamic balance appears to be untenable if the mean angle of attack is very small. Then an estimate must be made of the position of the center of lift for this angle of attack, and one of the analyses given in Appendix C should be tried with the hydrodynamic moment due to circulation included.

The simplified analysis would not be directly applicable to torsion-bending flutter of a control-surface member itself in which the hull did not play a significant role. This type of flutter might be encountered with activated antirolling fins. To apply the same basic analysis to such a system, the torsional and bending modes of the member must be reduced to an equivalent system of the apparatus type and the distributed forces and moments must be reduced to effective values which apply to the equivalent system. This method is frequently used in torsion-bending flutter of an aircraft wing in which the fuselage is considered fixed.

It appears feasible to develop a method of computation based on mechanical impedance of the hull as derived from digital calculations without using the normal concept. This method has not been explored up to the time of this writing.

Three-dimensional flow effects have been neglected in the analyses presented herein. The effects of finite aspect ratio on flutter are complex. Therefore three-dimensional flow effects are only occasionally used in flutter prediction. Discussions of these effects can be found in the references. The prevailing opinion in the aircraft field appears to be that three-dimensional effects are conservative and that the flutter speed is about 15 percent higher than that predicted by two-dimensional theory for moderate aspect ratios. The effect increases with small aspect ratio and decreases with large values of the reduced frequency ($b\omega/S$). However, the possibility that three-dimensional effects could be nonconservative cannot yet be ruled out.

SUGGESTIONS FOR FUTURE INVESTIGATIONS

A possible reason for the opinion that control-surface flutter effects are unlikely in the marine field is that naval architects are thinking in terms of classical aircraft wing flutter. Since it now appears that control-surface flutter phenomena, in the broad sense of the term, may be encountered in naval architecture, various aspects of flutter deserve further exploration.

On the hydrodynamic side, it is clear that much more information is needed on both the lift forces and moments on oscillating hydrofoils. Not only is an investigation of the validity of the steady, quasi-steady, or the classical (Theodorsen's) relations required; it is also important in this field to explore the region of small angles of attack and the range of Strouhal numbers much higher than those so far investigated in the aircraft field, It is particularly

desirable to establish the oscillatory hydrodynamic moment. Since the hydrodynamic moment arm L, as defined in this report on page 16, is indicated to be a nonlinear function of the angle of attack, the moment must also be a nonlinear function of attack angle.

The extent to which cavitation may affect such phenomena as occurred on DD 931 should be further investigated. Experimental flow studies on a series of foil shapes would be required, since the effects of cavitation can vary considerably with foil sectional shape, taper, and sweep.

As far as the rudder problem is concerned, this question must be answered: Does the use of a fixed skeg or horn forward of the rudder supporting a pintle bearing significantly raise a critical flutter speed?

On the structural side of the problem, it is important to establish the normal mode patterns of control-surface members in service and, particularly, to determine the relative magnitude of torsion and bending in their fundamental modes. If the trend in design is toward the spade-type rudder, then it would be helpful to investigate those features of the structural design which contribute to raising the critical speed. On the basis of the present study, there appear to be the following possibilities: (1) attaining mass balance, which is difficult because of the very large virtual mass effect; (2) increasing the torsional rigidity, which is determined only in part by the torsional stiffness of the rudder stock itself; and (3) using damping devices.

CONCLUSIONS

Control-surface flutter action has been demonstrated with the TMB flutter apparatus. Both the experiments and the analyses indicate that such a system may have a large variety of response characteristics for moderately small variations in the values of the design parameters. Thus, critically unstable and subcritical flutter action as well as stable conditions all appear possible in such a system. The same basic equations may be applied to a rudder-hull system, as pointed out on page 22.

With specific reference to rudder-hull systems (such as that of the DD 931 class), both the experiments and analyses indicate that the combination of downstream mass unbalance, close tuning of the two degrees of freedom, and ship speed can result in such a marked reduction in overall damping in the particular hull mode involved that usual sources of ship vibration produce intolerable hull amplitudes.

A complete flutter analysis of a control-surface system coupled with a mode of vibration of the entire hull would involve elaborate calculations based on the most advanced methods of structural mechanics and hydromechanics. However, simplified methods of analysis could well be used to obtain a preliminary indication of the possibility of either a critical flutter condition or a significant subcritical condition.

ACKNOWLEDGMENTS

The control-surface flutter project was a joint effort of the Hydromechanics and Structural Mechanics Laboratories of the David Taylor Model Basin. In the early planning stage and in the setting up of specifications for the design of the TMB flutter apparatus, Messrs. M.S. Macovsky of the Hydromechanics Laboratory and G.L. Santore of the Industrial Department made significant contributions. The design itself was made under the direction of Mr. E.D. Hoyt of Reed Research, Inc. under contract with the Model Basin. The apparatus was built in the TMB machine shop.

In the experiments in the towing basin and the subsequent analysis of the test data, the collaboration of LTJG A.J. Impink, USNR, was most helpful. He supervised the installation and calibration of the bulk of the instrumentation used on the high-speed carriage for these special tests. Mr. J.A. Luistro also supervised part of the test installation and, together with Mr. P.E. Strausser, furnished valuable assistance during the actual test runs.

In the analytical studies made under this project, valuable contributions were made by Miss R.A. Allan, Mrs. B.H. Gesswein, LTJG A.J. Impink, USNR, Mr. A.W. McIver, and Mrs. M. McG. Gillis, of the David Taylor Model Basin, and Messrs. W.P. Dewitt and B.G. Zimmerman of the Applied Mathematics Laboratory of the Naval Research Laboratory.

APPENDIX A

SUMMARY OF TEST DATA

The tests with the TMB Control-Surface Flutter Apparatus were of two types:

Series A. Runs with various settings of the mass unbalance and the nominal angle of attack during which there was no external stimulus aside from the normal carriage vibration, and the translational and rotational displacements of the apparatus were recorded on the oscillograph.

Series B. Impact tests in which the apparatus was excited by striking with a heavy timber while the towing carriage was under way, increasing speed at a very slow rate (not exceeding 0.15 knot/sec), and the subsequent vibrations were recorded.

The data obtained during the steady-speed runs (Series A) are summarized in Table 3. This summary includes all cases in which the amplitude in translation exceeded the noise level and without any adjustment for carriage vibration. A few cases with amplitudes less than the noise level are shown, to illustrate frequency variations. The double amplitudes in translation and rotation are $2\,Y_0$ and $2\,\theta_0$, respectively. These are the maxima observed in a given condition without correction for beating which occurred. Also in this table, ϕ is the phase angle by which the rotating time vector representing θ leads the vector representing Y. The values of ϕ tabulated are mean values and not values for specific cycles. Both the accuracy and the significance of the phase determination obviously increase with the extent of coupling, mh, of the two degrees of freedom.

In Table 4 are summarized the damping data derived from the impact tests (Series B).

TABLE 3 – Summary of Test Data Obtained during Steady-Speed Runs

Run No.	α_0 deg	$m\lambda$ lb-sec^2	S knots	f cps	$2Y_0$ in.	$2\theta_0$ radians	ϕ deg
11	0	0.3	4.87	3.73	0.041	0.0010	180
			4.87	3.94	0.050	0.0015	180
12		0.3	4.90	3.95	0.027	0.0008	180
			4.91	3.96	0.034	0.0010	170
			4.91	3.95	0.043	0.0012	170
14		1.8	9.15	4.02	0.048	0.0046	10
16		1.3	8.69	4.31	0.038	0.0038	60
18		0.8	8.60	4.23	0.037	0.0024	60
19		0.6	5.33	4.18	0.031	0.0016	45
20		0.2	4.78	3.88	0.051	0.0013	180
21		0.0	4.85	3.93	0.038	0.0010	180
22		−0.2	4.60	3.75	0.031	0.0009	− 90
23		−0.4	2.71	3.86	0.040	0.0025	− 60
			3.37	3.80	0.027	0.0015	− 90
			4.83	3.85	0.033	0.0018	−140
24		−0.6	2.58	3.83	0.025	0.0023	− 90
			4.81	3.90	0.027	0.0016	− 60
			7.70	3.75	0.023	0.0014	−120
25		−0.9	2.35	3.81	0.027	0.0029	− 60
			2.60	3.80	0.030	0.0031	− 50
			3.40	3.78	0.027	0.0022	− 60
			4.72	3.82	0.038	0.0030	− 90
27		2.0	5.60	4.45	0.027	0.0038	5
			9.40	4.59	0.039	0.0040	10
			10.40	4.62	0.032	0.0037	10
28			4.07	4.63	0.025	0.0035	–
			5.40	4.37	0.029	0.0044	10
			5.47	4.50	0.038	0.0055	10
			9.30	4.60	0.051	0.0055	60
			9.33	4.50	0.070	0.0077	70
			9.36	4.55	0.067	0.0056	60
39	2½	2.0	2.8	4.46	0.021	0.0028	0
			4.4	3.95	0.020	0.0027	90
			5.6	4.45	0.034	0.0031	0
			6.85	4.45	0.035	0.0031	0
			9.1	4.4	0.031	0.0028	5
40		1.8	2.1	4.0	0.019	0.0028	− 90
			3.18	4.5	0.026	0.0030	10
			4.6	4.45	0.028	0.0024	0
			9.35	4.55	0.039	0.0040	20
41		1.6	4.6	4.4	0.032	0.0033	0
			8.55	4.25	0.032	0.0024	50
			8.75	4.5	0.032	0.0025	70
42		1.3	3.65	4.22	0.027	0.0030	5
			4.4	4.4	0.028	0.0026	10
			5.4	4.23	0.033	0.0028	30
			6.8	4.4	0.024	0.0024	0
			9.0	4.35	0.023	0.0022	80
43		1.1	3.75	4.28	0.039	0.0031	25
			4.8	3.95	0.022	0.0021	110
			5.15	4.22	0.063	0.0023	0
			6.65	4.4	0.029	0.0019	50
44		0.8	3.7	4.20	0.029	0.0025	20
			6.44	4.18	0.030	0.0014	105
			6.47	4.22	0.040	0.0020	50
45		0.6	3.67	4.0	0.022	0.0011	60
			4.35	4.0	0.031	0.0012	30
			4.85	4.0	0.030	0.0013	75
			5.2	4.21	0.028	0.0013	60
46		0.3	3.86	3.9	0.036	0.0008	150
			4.85	3.9	0.044	0.0012	125
			5.4	4.02	0.031	0.0014	110
47		0.1	4.55	3.66	0.033	0.0008	–
48		0.0	4.7	3.9	0.027	0.0011	–
			8.15	4.0	0.024	–	–
58	5	2.0	3.97	4.3	0.022	0.0013	0
			7.0	4.5	0.035	0.0040	0
59	5	2.0	7.05	4.52	0.028	0.0025	10
			9.0	–	0.020	0.0014	45
60		1.8	6.6	4.27	0.020	–	–
			9.05	4.45	0.030	–	–
			9.33	4.53	0.020	–	20
61		1.6	8.4	4.12	0.021	0.0018	–
			9.00	4.38	0.019	0.0020	–
62		1.3	8.72	4.15	0.021	0.0017	45
			9.27	4.45	0.024	0.0014	0
63		1.1	8.65	4.25	0.021	0.0013	
			9.04	4.45	0.023	0.0010	–
65		0.6	6.2	4.0	0.030	0.0014	–
			8.09	4.0	0.028	0.0009	–
66		0.3	4.3	4.1	0.039	0.0012	–
			8.02	4.0	0.026	0.0008	–
67		0.2	4.9	4.00	0.034	0.0023	180
			8.10	4.0	0.019	0.0009	180
68		0.0	7.56	3.72	0.024	0.0008	− 90
			9.00	6.0	0.023	0.0008	−120
69		−0.4	7.5	3.63	0.026	0.0014	–
			8.44	4.0	0.027	0.0012	180
70		−0.8	5.5	3.55	0.031	0.0018	–
			7.24	3.65	0.030	0.0018	–
71		−0.9	4.5	3.6	0.049	0.0030	− 60
			7.30	3.61	0.027	0.0015	–
			7.61	3.70	0.019	0.0017	–
82	0	0.0	8.0	4.0	0.020	0.0015	–
83		2.0	4.65	4.48	0.024	0.0037	25
			5.58	4.48	0.042	0.0061	30
			7.0	4.49	0.036	0.0039	20
			9.5	4.57	0.039	0.0039	20
84		2.0	9.05	4.40	0.041	0.0050	60
			9.25	4.50	0.037	0.0041	30
			9.38	4.53	0.068	0.0067	30
			10.0	4.64	0.039	0.0041	45
			10.4	4.57	0.034	0.0037	35
87		2.0	13.75	4.5	0.064	0.0027	30
			17.35	4.3	0.068	0.0027	45
89		1.8	9.00	4.43	0.023	0.0026	50
			9.45	4.52	0.067	0.0031	90
90		1.6	9.00	4.40	0.046	0.0044	55
			9.00	4.35	0.050	0.0041	50
			9.02	4.36	0.050	0.0040	60
91		1.3	8.82	4.23	0.064	0.0065	–
			9.17	4.40	0.036	0.0050	70
92		1.1	8.88	4.37	0.021	0.0022	–
94		0.6	8.67	4.2	0.024	0.0018	130
95		0.3	8.59	4.22	0.025	0.0014	90
96		0.3	12.53	5.8/5.2*	0.039	0.0024	–
98	5	1.8	19.9	13.0	0.025	–	–
100		1.6	8.88	4.36	0.033	0.0028	–
101		1.3	8.81	4.26	0.033	0.0018	–
102		1.1	8.85	4.30	0.028	0.0018	110
103		1.1	15.9	13.2	0.023	0.0005	180
104		1.1	15.95	13.20	0.017	–	–
			19.20	12.45	0.014	–	–
			20.00	13.00	0.014	–	–
105	0	2.0	3.96	4.5	0.054	0.0038	0
107		2.0	9.35	4.5	0.049	0.0049	–
109		0.0	4.9	4.0	0.047	0.0010	180
114		0.0	3.93	3.84	0.041	0.0010	–
			8.50	4.30	0.031	0.0021	180
115		2.0	9.28	4.5	0.056	0.0052	20
116		2.0	9.3	4.53	0.058	0.0064	10
117		2.0	9.32	4.49	0.050	0.0055	25

*The translational and rotational frequencies differ.

TABLE 4 – Summary of Damping Data Derived from Impact Tests

α_0 = 0 degrees.

Run No.	mh lb-sec^2	Translational or Rotational	S knots	f cps	DR	ϕ deg
13	0.3	Translational	3.9	4.0	0.064	120
			4.9	3.9	0.075	120
			6.1	4.1	0.082	165
			6.9	–	0.081	–
			8.1	–	0.095	–
			8.9	4.0	0.110	175
		↓	9.7	4.4	0.122	160
109	0.0	Translational	4.0	4.0	0.086	–
			6.3	4.0	0.126	–
			9.1	4.1	0.141	–170
		↓	10.0	–	0.143	–
105	2.0	Translational	4.2	4.5	0.011	0
		Rotational	4.2	4.5	0.011	0
		Translational	4.7	4.5	0.012	0
		Translational	4.9	4.5	0.012	0
		Rotational	4.9	4.5	0.011	0
		Translational	5.5	4.5	0.008	0
		Rotational	5.5	4.5	0.009	0
		Translational	6.0	4.5	0.013	0
		Rotational	6.0	4.5	0.013	0
		Translational	6.4	4.5	0.015	0
		Rotational	6.4	4.5	0.014	0
		Translational	6.6	4.5	0.022	0
		Rotational	6.6	4.5	0.022	0
		Translational	6.7	4.5	0.019	0
		Rotational	6.7	4.5	0.019	0
		Translational	6.8	4.5	0.020	0
		Rotational	6.8	4.5	0.022	0
		Translational	7.2	4.5	0.025	0
		Rotational	7.2	4.5	0.019	0
		Translational	7.6	4.5	0.013	0
		Rotational	7.6	4.5	0.015	0
		Translational	8.5	4.5	0.020	15
		Rotational	8.5	4.5	0.016	15
		Translational	9.1	4.5	0.018	0
		Rotational	9.1	4.5	0.023	0
		Rotational	9.6	4.5	0.013	0
		Translational	9.8	4.6	0.016	0
		Translational	10.1	4.6	0.046	0
		Rotational	10.1	4.6	0.040	0
106	2.0	Rotational	10.7	4.6	0.031	10
		Translational	10.8	4.5	0.027	10
		Rotational	11.3	4.6	0.034	10
		Rotational	11.9	4.4	0.046	10
		Translational	12.1	4.5	0.035	20
		Rotational	12.5	4.4	0.040	10
			12.7	4.6	0.036	10
			13.3	–	0.069	10
		↓	14.7	–	0.048	10

APPENDIX B

SIMPLIFIED ANALYSIS INITIALLY APPLIED TO TMB FLUTTER APPARATUS

For the simplified analysis, the TMB flutter apparatus may be represented schematically by the plan view shown in Figure 8.

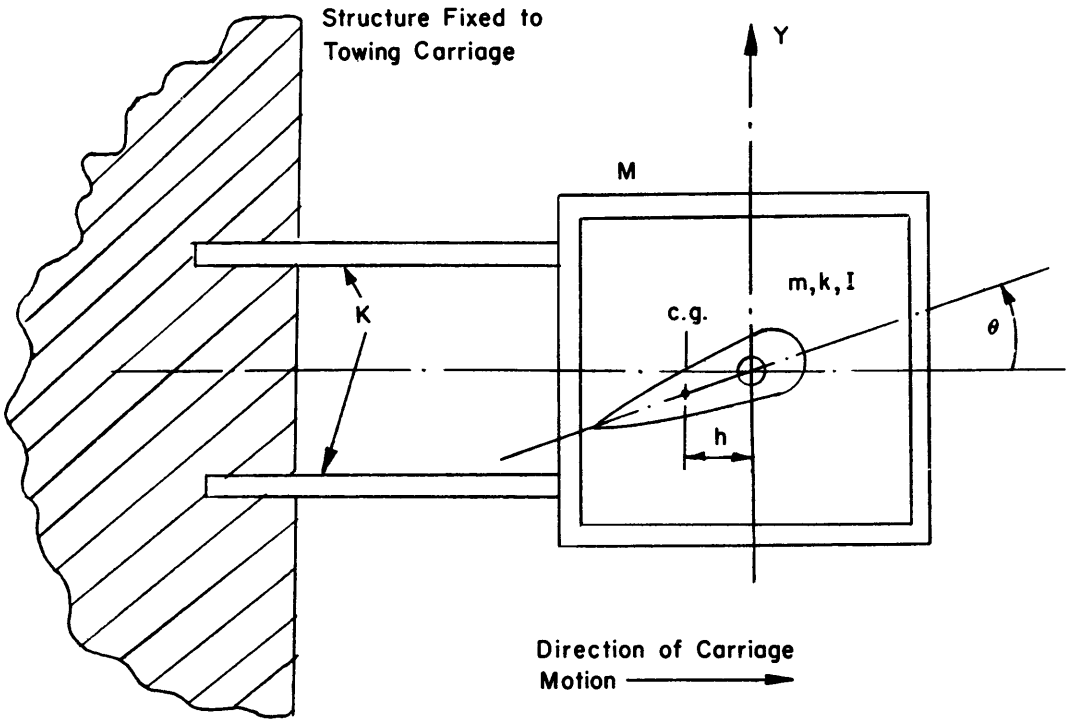

Figure 8 – Schematic Plan View of TMB Flutter Apparatus

In this figure, θ is greatly exaggerated. For small values of θ, h as shown is approximately the same as the distance measured along the chord. The torsion spring k connecting the rotational and translation elements is not shown.

The symbols used in Figure 8 are defined in Table 1 except for Y and θ, which are the horizontal displacement of the axis of the hydrofoil and the angular displacement of the hydrofoil, respectively. If the towing speed S is in the direction indicated in Figure 8, then, since the velocity of the water relative to the hydrofoil is in the opposite direction, the effective angle of attack is:

$$\alpha = \theta - \frac{\dot{Y}}{S}$$

If the lift force under oscillatory motion follows the nonoscillatory or steady relation, this force F_L is given by the relation

$$F_L = A S^2 \alpha$$

where A is defined in Table 1. Equations of motion can be written relative to a set of coordinates moving in translation with the hydrofoil axis, provided an additional fictitious force equal to $-m\ddot{Y}$ is applied at the center of mass of the hydrofoil. Hence, if under oscillatory motion the center of lift remains at the axis of rotation, as assumed for hydrodynamic balance, the equation for the angular motion becomes

$$I\ddot{\theta} + c\dot{\theta} + k\theta = m\ddot{Y}h$$

The moments due to water inertia and damping effects at zero speed are assumed included here in the evaluation of I and c, respectively.

In simple harmonic oscillations

$$\ddot{Y} = -Y\omega^2$$

and the steady-state solution for θ may be expressed in the complex form:

$$\theta = \frac{-m Y \omega^2 h}{k - I\omega^2 + jc\omega}$$

If the frequency corresponds to the torsional natural frequency of the hydrofoil,

$$\omega^2 = \frac{k}{I}$$

and

$$\theta = \frac{-m Y \omega^2 h}{jc\omega} = \frac{jm\omega h Y}{c}$$

The lift force is $A(S^2\theta - \dot{Y}S)$. The force required to accelerate the rudder in the Y-direction is $m\ddot{Y}_{c.g.}$, but

$$Y_{c.g.} = Y - h\theta$$

and

$$\ddot{Y}_{c.g.} = \ddot{Y} - h\ddot{\theta}$$

also

$$\ddot{\theta} = \frac{j m h \omega}{c} \ddot{Y};$$

therefore

$$\ddot{Y}_{c.g.} = \ddot{Y} \left(1 - \frac{j m h^2 \omega}{c}\right)$$

Thus, the effective force on the nonrotating element is:

$$P_0 = A (S^2 \theta - \dot{Y} S) - m \ddot{Y} \left(1 - \frac{j m h^2 \omega}{c}\right)$$

Hence

$$P_0 = \frac{j A S^2 m h \omega Y}{c} - A \dot{Y} S - m \ddot{Y} + \frac{j m^2 h^2 \omega}{c} \ddot{Y}$$

If the mass of the nonrotating element is M, the translational damping constant C, and the translational spring constant K, the equation for oscillatory motion of M becomes

$$M \ddot{Y} + C \dot{Y} + K Y = \frac{j A S^2 m h Y \omega}{c} - A \dot{Y} S - m \ddot{Y} + j \frac{m^2 h^2 \omega \ddot{Y}}{c}$$

which yields the equation:

$$(M + m) \ddot{Y} + \left(C - \frac{A S^2 m h}{c} + A S + \frac{m^2 h^2 \omega^2}{c}\right) \dot{Y} + K Y = 0$$

It is seen that if the coefficient of $\dot{Y}$ is positive, this is the equation for damped free oscillations of a mass $(M + m)$. If, however, this coefficient is negative, such an equation indicates that a self-excited or unstable oscillation is possible.

It is essential to note that this equation was derived on the assumption that oscillations are possible at the frequency

$$\omega = \sqrt{\frac{k}{I}} = \sqrt{\frac{K}{M + m}}$$

If the damping is large this would not be possible, but the equation is used only in deriving a speed at which the overall damping vanishes.

It should be noted that the only negative term in the coefficient of $\dot{Y}$ contains S^2. Hence it is clear that there will be some speed beyond which the coefficient will be negative, and the speed at which it becomes zero would be designated the flutter speed.

The equation

$$C - \frac{AS^2mh}{c} + AS + \frac{m^2h^2\omega^2}{c} = 0$$

yields the curve plotted in Figure 6a (indicated as $L = 0$) giving the flutter speed in terms of the mass unbalance mh, as predicted by this simplified analysis. The positive value of S given by this equation is

$$S = \frac{c}{2mh} + \sqrt{\frac{c^2}{4m^2h^2} + \frac{c}{Amh}\left[C + \frac{m^2h^2\omega^2}{c}\right]}$$

From the manner in which the equation for oscillatory motion of M on page 33 was derived, it is clear that the coefficient of $\dot{Y}$ can be used in plotting overall damping as a function of S only in the range of speeds in which the overall damping is very small, since ω is not actually independent of damping.

APPENDIX C

FURTHER METHODS OF FLUTTER ANALYSIS

The development of the extended simplified analysis and the modified Theodorsen analysis are outlined below, together with the method of solution used.

The motions of the apparatus shown diagrammatically in Figure 8 can be described by the following pair of ordinary differential equations

$$I\ddot{\theta} + c\dot{\theta} + k\theta - mh\ddot{Y} = M_\theta$$

$$(M + m)\ddot{Y} + C\dot{Y} + KY - mh\ddot{\theta} = F_L$$

The constants, as previously defined, include both added inertia and zero speed hydrodynamic damping effects. M_θ is the fluid dynamic moment about the axis of rotation, and F_L is the fluid dynamic lift force. In this notation, M_θ and F_L do not include added mass or zero speed hydrodynamic damping effects. Coincidence of the rotational and translational natural frequencies was not assumed in deriving these equations. They yield the simplified analysis if $M_\theta = 0$, $F_L = AS^2\left(\theta - \frac{\dot{Y}}{S}\right)$ and $\omega^2 = \frac{K}{M+m} = \frac{k}{I}$. Further development of the extended simplified analysis and the modified Theodorsen analysis consists merely of using two other real expresssions for M_θ and F_L in these general equations.

EXTENDED SIMPLIFIED ANALYSIS

In this analysis, terms were introduced to account for the effect of a hydrodynamic moment (in addition to the added mass moment of inertia and angular damping effects obtained at zero speed). The expedient used was the assignment of a value to the distance L of the center of lift from the axis so that the product of the lift force and L would give the required moment. It was assumed here that the oscillatory moment, as well as the oscillatory lift force, follows the steady relations with respect to both speed and angle of attack. Since the oscillatory lift force is given by

$$F_L = AS^2\left(\theta - \frac{\dot{Y}}{S}\right)$$

this moment is written

$$M_\theta = ALS^2\left(\theta - \frac{\dot{Y}}{S}\right)$$

Upon substituting the above values for M_θ and F_L, the equations of motion become:

$$I\ddot{\theta} + c\dot{\theta} + (k - ALS^2)\,\theta - mh\ddot{Y} + ALS\dot{Y} = 0$$

$$-mh\ddot{\theta} - AS^2\theta + (M + m)\,\ddot{Y} + (C + AS)\,\dot{Y} + KY = 0$$

It can be seen that the moment terms proportional to L signify a negative hydrodynamic restoring effect as well as coupling between the translational and rotational degrees of freedom. If simple harmonic motions are possible in this system, they can be represented by $\theta = \theta_0 e^{\lambda t}$, $Y = Y_0 e^{\lambda t}$ where θ_0, Y_0, and λ are complex. Then the following pair of algebraic equations must be satisfied:

$$(I\lambda^2 + c\lambda + k - ALS^2)\,\theta_0 + (-mh\lambda^2 + ALS\lambda)\,Y_0 = 0$$

$$(-mh\lambda^2 - AS^2)\,\theta_0 + [(M + m)\,\lambda^2 + (C + AS)\,\lambda + K]\,Y_0 = 0$$

A nontrivial solution is possible only if the determinant of the coefficients vanishes. Thus:

$$\begin{vmatrix} I\lambda^2 + c\lambda + k - ALS^2 & -mh\lambda^2 + ALS\lambda \\ -mh\lambda^2 - AS^2 & (M + m)\lambda^2 + (C + AS)\lambda + K \end{vmatrix} = 0$$

The expansion of this determinant gives the following quartic equation in the complex frequency:

$$[I(M + m) - (mh)^2]\,\lambda^4 + [IC + (M + m)c + A(I + mhL)S]\lambda^3$$

$$+ [IK + Cc + k(M + m) + AcS - A(\{M + m\}L + mh)\,S^2]\lambda^2$$

$$+ [Kc + kC + AkS - ALCS^2]\,\lambda + Kk - KALS^2 = 0$$

If $\lambda = j\omega = j\sqrt{\frac{k}{I}} = j\sqrt{\frac{K}{M + m}}$ and $L = 0$, this frequency quartic can be reduced to the equation obtained by setting the damping coefficient given in Appendix B equal to zero.

MODIFIED THEODORSEN ANALYSIS

The oscillatory force and moment on a vibrating foil were obtained by Theodorsen[10] in a classical analysis. He expressed the force and moment per unit length of foil in terms of the rectilinear and angular displacements and their time derivatives, as well as the Strouhal

number and the distance from midchord to the axis of rotation. His expressions contain terms for the effects of added inertia. After omitting the latter terms, multiplying by the foil length l, and inserting the value of the distance from midchord to the axis of rotation, the oscillatory force and moment appropriate to the TMB flutter apparatus become:

$$F_L = \pi \rho\, b^2 l\, [S\,\dot{\theta}] + 2\pi \rho\, l\, b\, C_k\, S\, [S\,\theta - \dot{Y} + b\,\dot{\theta}]$$

$$M_\theta = -\pi \rho\, l\, b^2\, [S\, b\,\dot{\theta}]$$

where ρ is the mass density of the fluid and C_k is the complex Theodorsen function. In general, the terms involving C_k represent the forces and moments due to circulation. It is noted that if the axis of rotation is at the forward quarterchord location, the moment due to circulation is zero in these expressions. In general, the circulatory moment is not zero. The product of constants $2\pi \rho\, l\, b$ is equivalent to the lift constant A previously defined. For very low reduced frequencies (0.00 – 0.02), Theodorsen's function is equated to unity under the quasi-steady assumption frequently used in aeroelasticity. A similar assumption is used here. In both of these assumptions, the absolute value of C_k is approximately preserved; however, the small phase lag due to the imaginary component is neglected. Since the reduced frequency of the apparatus is relatively high (of the order of 1.2 at S = 9 knots), the value of C_k was equated to one-half. (See Figure 5.20 of Reference 7.) The reduced expressions for lift and moment can now be written:

$$F_L = \frac{1}{2} AS^2\,\theta - \frac{1}{2} A\, S\,\dot{Y} + A\, b\, S\,\dot{\theta}$$

$$M_\theta = -\frac{1}{2} A\, b^2 S\,\dot{\theta}$$

The problem of how best to express the oscillatory moment due to circulation arose in this analysis. Previously, the expression $L\,F_L$ was used. It appeared that perhaps the use of L to modify all the unsteady lift terms was excessive, considering that at this stage it is meant to be a simple expedient. It was thought that the oscillatory moment due to circulation might better be expressed as $\frac{1}{2}\, A\, L\, S^2\theta$, taking only the θ dependent term and neglecting the lift terms proportional to $\dot{Y}$ and $\dot{\theta}$. No guidance on this problem was found in the literature on flutter. Therefore two exploratory sets of calculations were made, one using the full expression $L\,F_L$ and the other using just the single term. The resultant critical frequencies obtained with the use of the full expression for a large value of L were considered too unrealistic to be usable. The problem was therefore deferred and the one-term expression was used for the remainder of this work. A separate investigation at the Model Basin to obtain a method of representing the oscillatory moment due to circulation has been started on the basis of this unresolved problem.

The total moment including the moment due to circulation can now be written:

$$M_\theta = -\frac{1}{2} A b^2 S \dot{\theta} + \frac{1}{2} A L S^2 \theta$$

At this point, a comparison of these expressions with those used for the extended simplified analysis should be profitable. The term $A b S \dot{\theta}$ in F_L, containing forces both circulatory and noncirculatory in origin, represents additional coupling of the degrees of freedom. The term $-\frac{1}{2} A b^2 S \dot{\theta}$ in the moment expression represents dynamic damping which was previously neglected. The circulatory moment term $-A L S \dot{Y}$ used previously has no counterpart here. Upon substitution of the expressions for F_L and M_θ, the equations of motion become:

$$I \ddot{\theta} + \left(c + \frac{1}{2} A b^2 S\right) \dot{\theta} + \left(k - \frac{1}{2} A L S^2\right) \theta - mh \ddot{Y} = 0$$

$$-mh \ddot{\theta} - A b S \dot{\theta} - \frac{1}{2} A S^2 \theta + (M + m) \ddot{Y} + \left(C + \frac{1}{2} A S\right) \dot{Y} + KY = 0$$

Thus, because of the simplifying assumptions, the equations of motion again have real coefficients. By assuming simple harmonic motion, the equations can be reduced to:

$$\left[I\lambda^2 + k - \frac{1}{2} A L S^2 + \left(c + \frac{1}{2} A b^2 S\right)\lambda\right] \theta_0 + \left[-mh\lambda^2\right] Y_0 = 0$$

$$\left[-mh\lambda^2 - A b S \lambda - \frac{1}{2} A S^2\right] \theta_0 + \left[(M + m)\lambda^2 + \left(C + \frac{1}{2} A S\right)\lambda + K\right] Y_0 = 0$$

The determinant of the coefficients is again equated to zero and expanded to obtain the complex frequency equation:

$$\left[I(M + m) - (mh)^2\right]\lambda^4 + \left[(M + m)\left(c + \frac{1}{2} A b^2 S\right) + I\left(C + \frac{1}{2} A S\right) - A b mh S\right] \lambda^3$$

$$+ \left[(M + m)\left(k - \frac{1}{2} A L S^2\right) + \left(C + \frac{1}{2} A S\right)\left(c + \frac{1}{2} A b^2 S\right) + IK - \frac{1}{2} A mh S^2\right] \lambda^2$$

$$+ \left[\left(C + \frac{1}{2} A S\right)\left(k - \frac{1}{2} A L S^2\right) + K\left(c + \frac{1}{2} A b^2 S\right)\right] \lambda + K\left(k - \frac{1}{2} A L S^2\right) = 0$$

SOLUTION OF POLYNOMIAL EQUATIONS

The frequency quartic (obtained in either of these analyses) was rewritten:*

$$\lambda^4 + A_3\lambda^3 + A_2\lambda^2 + A_1\lambda + A_0 = 0$$

The A's thus defined are functions of S. At any given speed, the quartic will have four complex roots of the form $\lambda = \mu + j\omega$. Thus the time dependent displacements will be $Y = Y_0\, e^{\mu t} e^{j\omega t}$ and $\theta = \theta_0\, e^{\mu t} e^{j\omega t}$. The circular frequency of vibration is ω. If μ is positive, the oscillation is unstable; if negative, the oscillation is stable. At neutral stability, $\mu = 0$ and the root is a pure imaginary. It can be shown that for stability it is necessary that all of the A's be greater than zero and also that $A_1 A_2 A_3 - A_1^2 - A_0 A_3^2$ be positive.** The condition $A_0 = 0$ gives the divergence speed for which $\lambda = 0$. The quantity $D = A_1A_2A_3 - A_1^2 - A_0A_3^2$ is the Routh discriminant, which is also a function of S. If all the A's are positive, the critical flutter speed is the speed at which $D(S) = 0$. There can be multiple critical speeds separating stable and unstable ranges. At any critical speed, $\omega^2 = A_1/A_3$. The values A_0, A_1, A_2, A_3, and D were computed as functions of speed for various values of L and mh on a digital computer. In nearly every case, D equaled zero at a lower speed than that at which any value of A was equal to zero. In those cases, the condition $D = 0$ is equivalent to zero net system damping. Thus, the critical speeds and frequencies were obtained. Summaries of the critical flutter calculations based on the extended simplified analysis and the modified Theodorsen analysis are shown in Tables 5 and 6, respectively.

---

*The A's with subscripts are not to be confused with the lift coefficient A without a subscript.

**See page 119 of Reference 7.

TABLE 5

Summary of Critical Flutter Calculations Based on Extended Simplified Analysis

mh lb-sec^2	S knots	f cps	mh lb-sec^2	S knots	f cps
L = 0.0 in.			L = 8.9 in.		
0.2	7.10	3.89	−1.0	3.83	4.11
0.4	5.86		−0.8	4.05	4.06
0.6	6.12		−0.6	4.80	4.02
0.8	6.56		2.0	4.65	3.51
1.0	7.12			5.91	3.51
1.2	7.60		2.2	4.35	3.50
1.4	8.13			6.40	3.47
1.6	8.58		2.4	4.20	3.45
1.8	9.08			7.02	3.41
2.0	9.48		2.6	4.10	3.43
2.2	9.96			7.29	3.37
2.4	10.33		2.8	4.03	3.40
2.6	10.73			7.63	3.40
2.8	11.13		3.0	3.98	3.33
3.0	11.47			8.02	3.06
L = 2.8 in.			L = 10.0 in.		
0.2	7.74	3.87	−1.0	2.44	4.10
0.4	6.12	3.86	−0.8	2.54	4.06
0.6	6.24	3.84	−0.6	2.83	4.02
0.8	6.64	3.83	−0.4	3.69	3.97
1.0	7.14	3.81	1.2	3.14	3.64
1.2	7.56	3.80		4.67	3.61
1.4	8.06	3.78	1.4	2.88	3.61
1.6	8.44	3.77		5.41	3.57
1.8	8.88	3.75	1.6	2.76	3.58
2.0	9.24	3.74		6.07	3.52
2.2	9.60	3.72	1.8	2.68	3.56
2.4	10.00	3.71		6.44	3.48
2.6	10.29	3.70	2.0	2.63	3.53
2.8	10.61	3.68		6.94	3.43
3.0	10.95	3.67	2.2	2.59	3.49
L = 6.41 in.				7.24	3.39
			2.4	2.57	3.47
2.0	15.00	3.54		7.54	3.35
2.2	13.46	3.52	2.6	2.55	3.44
	17.32	3.50		7.89	3.32
2.4	13.35	3.49	2.8	2.53	3.41
	18.29	3.47		8.14	3.28
2.6	13.39	3.39	3.0	2.52	3.38
	19.40	3.44		8.36	3.25
2.8	13.50	3.40			
3.0	13.62	3.41			

TABLE 6

Summary of Critical Flutter Calculations Based on Modified Theodorsen Analysis

mh lb-sec^2	S knots	f cps	mh lb-sec^2	S knots	f cps
L = 0.0 in.			L = 8.05 in.		
1.8	16.01	4.27	2.0	12.98	4.11
2.0	14.14	4.31		13.88	4.01
2.2	13.29	4.36	2.2	11.22	4.19
2.4	12.90	4.41		17.43	4.00
2.6	12.70	4.46	2.4	10.82	4.26
2.8	12.65	4.52		19.47	3.96
3.0	12.69	4.58	2.6	10.69	4.32
L = 2.8 in.			2.8	10.68	4.37
			3.0	10.75	4.43
1.6	19.85	4.07	L = 10.0 in.*		
1.8	13.64	4.19			
2.0	12.40	4.25	2.2	11.97	4.14
2.2	11.89	4.30		13.30	4.10
2.4	11.64	4.35	2.4	10.91	4.23
2.6	11.56	4.40	2.6	10.63	4.28
2.8	11.58	4.46	2.8	10.65	4.34
3.0	11.67	4.52	3.0	10.59	4.39

*Divergence speed at 16.0 knots.

REFERENCES

1. Antkowiak, E.T., "Hull Vibration in the DD 931 Class Destroyer," Boston Naval Shipyard Evaluation Report No. R-10 (20 Aug 1956).

2. Macovsky, M.S., et al., "An Investigation of a Flow-Excited Vibration of the USS FORREST SHERMAN (DD 931)," David Taylor Model Basin Report 1188 (Aug 1958).

3. Bureau of Ships letter S 87(442) Ser 442-107 of 9 Oct 1956 to David Taylor Model Basin.

4. Lankester, S.G. and Wallace, W.D., "Some Investigations into Singing Propellers," N.E.C.I. Transactions, Vol. 71, Part 7 (1955).

5. Taylor, J. Lockwood, "Propeller Blade Vibration," T.I.N.A., Vol. 85 (1943).

6. Wilson, W. Ker, "A Review of Ship Vibration Problems," The Marine Engineer and Naval Architect (Jul, Aug, Oct, and Nov 1955). Also published in American Society of Naval Engineers Journal (May 1954).

7. Scanlan, R.H. and Rosenbaum, R., "Introduction to the Study of Aircraft Vibration and Flutter," MacMillan Company, New York (1951).

8. Bisplinghoff, R.L., et al., "Aeroelasticity," Addison-Wesley Publishing Company, Cambridge, Mass. (1955).

9. Fung, Y.C., "An Introduction to the Theory of Aeroelasticity," John Wiley & Sons, Inc., New York (1955).

10. Theodorsen, T., "General Theory of Aerodynamic Instability and the Mechanism of Flutter," National Advisory Committee for Aeronautics Report 496 (1934).

11. Frazer, R.A., et al., "Elementary Matrices," MacMillan Company, New York (1947).

12. Wright, E.A., CAPT, USN, "New Research Resources at the David Taylor Model Basin," presented at the Spring Meeting, Society of Naval Architects and Marine Engineers (June 1958). Also reproduced as David Taylor Model Basin Report 1292 (Jan 1959).

13. Reed Research, Inc., "Design Calculations for Rudder Vibration Test Gear," Contract NObs 66059, Task Order No. 19, to David Taylor Model Basin, Project RR-1097 X (Feb 1957).

14. Saunders, H.E., "Hydrodynamics in Ship Design," published by The Society of Naval Architects and Marine Engineers, New York (1957).

15. Von Kármán, Theodor and Biot, Maurice A., "Mathematical Methods in Engineering," McGraw-Hill Book Company, New York (1940).

16. Dryden, H.L., et al., "Hydrodynamics," Dover Publications, Inc., New York (1956).

17. McGoldrick, R.T., et al., "Recent Developments in the Theory of Ship Vibration," David Taylor Model Basin Report 739 (Feb 1951).

BIBLIOGRAPHY

1. Abramson, H.N. and Chu, W.H., "A Discussion of the Flutter of Submerged Hydrofoils," Southwest Research Institute Report 1, Contract No. NOnr 2470(00), SWRI Project 19-754-2 (Aug 1958).

2. Czaykowski, T., "Definitions of Damping in Aircraft Response," Aircraft Engineering, Vol. XXX, No. 354 (Aug 1958).

3. Flax, A.H., "Aero-and-Hydro-Elasticity," First Symposium on Naval Structural Mechanics, Stanford University, Stanford, California (Aug 1958).

4. Heller, S.R., Jr., CDR, USN, and Abramson, H.N., "Hydroelasticity: A New Naval Science," First Symposium on Naval Structural Mechanics, Stanford University, Stanford, California (Aug 1958).

5. Henry, C.J., et al., "Aeroelastic Stability of Lifting Surfaces in High-Density Fluids," Journal of Ship Research, Vol. 2, No. 4 (Mar 1959).

6. Krivtsov, Y.V. and Pernik, A.J., "The Singing of Propellers" ("Penie Grebnykh Vintov"), Sudostroeniye, No. 10 (Oct 1957). Also published as David Taylor Model Basin Translation 281, by B.V. Nakonechny (Oct 1958).

7. Leibowitz, R.C., "Modes of Vibration of Rudder of USS ALBACORE (AGSS 569)," David Taylor Model Basin Report C-952 (Feb 1959) CONFIDENTIAL.

8. Leibowitz, R.C. and Kennard, E.H., "The Theory of Freely Vibrating Nonuniform Beams Including Methods of Solution and Application to Ships," David Taylor Model Basin Report 1317 (in preparation).

INITIAL DISTRIBUTION

Copies	
13	CHBUSHIPS 3 Tech Info Sec (Code 335) 1 Tech Asst to Chief (Code 106) 2 Appl Science (Code 340) 1 Design (Code 410) 1 Prelim Design (Code 420) 2 Hull Design (Code 440) 3 Submarines (Code 525)
5	CHBUORD, Underwater Ord (Re6a) 1 Dr. A. Miller 1 Mr. H.A. Eggers
3	CHBUAER 2 Aero & Hydro Br (DE-3) 1 Appl Math Br
4	CHONR 1 Math Br (Code 432) 2 Mech Br (Code 438) 1 Undersea Br (Code 466)
2	NAVSHIPYD MARE
2	NAVSHIPYD NORVA
2	NAVSHIPYD PTSMH
2	NAVSHIPYD BSN
2	NAVSHIPYD NYK
2	NAVSHIPYD PHILA
2	NAVSHIPYD CHASN
2	NAVSHIPYD LBEACH
2	NAVSHIPYD SFRAN
2	NAVSHIPYD PUG
2	NAVSHIPYD PEARL
2	DIR, USNRL
4	CDR, USNOL, Mech Div, White Oak
2	CDR, USNOTS, China Lake 1 Underwater Ord Div, Pasadena
1	CDR, USNPG
1	CO & DIR, USNUSL
2	CO, USNUOS, Design Sec
1	SUPT, USNAVPGSCOL
1	Dir, Marine Physical Lab, USNEL
1	SUPSHIPINSORD, Bath
1	SUPSHIPINSORD, Quincy
1	SUPSHIPINSORD, New York
1	SUPSHIPINSORD, Camden
1	SUPSHIPINSORD, Newport News
1	SUPSHIPINSORD, Pasacagoula
1	SUPSHIPINSORD, New Orleans
1	SUPSHIPINSORD, Great Lakes
1	SUPSHIPINSORD, Long Beach
1	SUPSHIPINSORD, San Francisco
1	SUPSHIPINSORD, Seattle
1	SUPSHIPINSORD, Elec Boat Div, Groton

Copies	
1	SUPT, USNA
1	CO, USNROTC & NAVADMINU MIT
1	CO, USFTC, Norfolk
1	CO, USNAVADUSEAWPNSCOL
1	CO, USNADMC, Attn: NADC Library
1	CO, USNAF, China Lake
1	CO, USNAOTS, Chincoteague
1	CO, USNOL, Corona
1	CO, USNOU, Key West
1	ONR, Boston
1	ONR, Chicago
1	ONR, London
1	ONR, New York
1	ONR, Pasadena
1	ONR, San Francisco
1	O in C, PGSCOL, Webb
1	Dir of Def (R & E)
1	NRC
2	CDR, ASTIA
1	DIR, Aero Res Lab, W-PAFB
1	DIR, NASA
4	DIR, Langley Res Ctr, NASA 1 Dr. A.E. von Doenhoff 1 Mr. N. Tetervin 1 Hydro Div
2	DIR, Lewis Res Ctr, NASA
2	DIR, Ames Res Ctr, NASA
1	CDR, AF Cambridge Res Ctr Attn: CRQSR-1
1	CDR, ARESDEVCOM Attn: RDSTIL
1	CDR, ARESDEVCOM, WDEVDIV Attn: WDSOT
1	BAGR, W-PAFB, Attn: BAU-ADD
1	CDR, W-PADEVCEN
1	DIR, Ballistic Res Lab, APG
1	DIR, Tech Info Br, APG
1	CHF, Appl Nav Arch, USMMA
1	ADMIN, Maritime Admin
1	COMDT, USCG
2	DIR, Natl BuStand 1 Chief, Natl Hydraulic Lab
1	DIR, Op Res Off, Bethesda
1	OTS, Dept Com, Attn: Tech Rpt Sec
8	ALUSNA

David Taylor Model Basin. Report 1222.
A CONTROL-SURFACE FLUTTER STUDY IN THE FIELD OF NAVAL ARCHITECTURE, by R.T. McGoldrick and D.A. Jewell. September 1959. v, 45p. illus., photos., graphs, tables, refs. UNCLASSIFIED

This study of control-surface flutter was initiated because of serious hull vibration on destroyers of the DD 931 Class. The source of the vibration had been traced to the twin rudders by the Boston Naval Shipyard.

For making experimental observations on control-surface flutter phenomena in the towing basin, the David Taylor Model Basin constructed the TMB Control-Surface Flutter Apparatus. With this equipment, a marked decrease in overall damping was demonstrated when the downstream mass unbalance was increased during underway tests.

1. Control surfaces – Flutter – Mathematical analysis
2. Control surfaces – Flutter – Test methods
3. Ship hulls – Vibration – Sources

I. McGoldrick, Raymond T.
II. Jewell, David A.
III. NS 715-090

David Taylor Model Basin. Report 1222.
A CONTROL-SURFACE FLUTTER STUDY IN THE FIELD OF NAVAL ARCHITECTURE, by R.T. McGoldrick and D.A. Jewell. September 1959. v, 45p. illus., photos., graphs, tables, refs. UNCLASSIFIED

This study of control-surface flutter was initiated because of serious hull vibration on destroyers of the DD 931 Class. The source of the vibration had been traced to the twin rudders by the Boston Naval Shipyard.

For making experimental observations on control-surface flutter phenomena in the towing basin, the David Taylor Model Basin constructed the TMB Control-Surface Flutter Apparatus. With this equipment, a marked decrease in overall damping was demonstrated when the downstream mass unbalance was increased during underway tests.

1. Control surfaces – Flutter – Mathematical analysis
2. Control surfaces – Flutter – Test methods
3. Ship hulls – Vibration – Sources

I. McGoldrick, Raymond T.
II. Jewell, David A.
III. NS 715-090

David Taylor Model Basin. Report 1222.
A CONTROL-SURFACE FLUTTER STUDY IN THE FIELD OF NAVAL ARCHITECTURE, by R.T. McGoldrick and D.A. Jewell. September 1959. v, 45p. illus., photos., graphs, tables, refs. UNCLASSIFIED

This study of control-surface flutter was initiated because of serious hull vibration on destroyers of the DD 931 Class. The source of the vibration had been traced to the twin rudders by the Boston Naval Shipyard.

For making experimental observations on control-surface flutter phenomena in the towing basin, the David Taylor Model Basin constructed the TMB Control-Surface Flutter Apparatus. With this equipment, a marked decrease in overall damping was demonstrated when the downstream mass unbalance was increased during underway tests.

1. Control surfaces – Flutter – Mathematical analysis
2. Control surfaces – Flutter – Test methods
3. Ship hulls – Vibration – Sources

I. McGoldrick, Raymond T.
II. Jewell, David A.
III. NS 715-090

David Taylor Model Basin. Report 1222.
A CONTROL-SURFACE FLUTTER STUDY IN THE FIELD OF NAVAL ARCHITECTURE, by R.T. McGoldrick and D.A. Jewell. September 1959. v, 45p. illus., photos., graphs, tables, refs. UNCLASSIFIED

This study of control-surface flutter was initiated because of serious hull vibration on destroyers of the DD 931 Class. The source of the vibration had been traced to the twin rudders by the Boston Naval Shipyard.

For making experimental observations on control-surface flutter phenomena in the towing basin, the David Taylor Model Basin constructed the TMB Control-Surface Flutter Apparatus. With this equipment, a marked decrease in overall damping was demonstrated when the downstream mass unbalance was increased during underway tests.

1. Control surfaces – Flutter – Mathematical analysis
2. Control surfaces – Flutter – Test methods
3. Ship hulls – Vibration – Sources

I. McGoldrick, Raymond T.
II. Jewell, David A.
III. NS 715-090

A condition in which hydrofoil oscillatory motion results in low damping without oscillatory instability is defined as "subcritical flutter." Such a condition, which greatly magnifies the sensitivity of the mechanical system to external sources of vibration, may be quite significant in the field of naval architecture. Analyses varying in complexity are explored and compared with experimental results.

A condition in which hydrofoil oscillatory motion results in low damping without oscillatory instability is defined as "subcritical flutter." Such a condition, which greatly magnifies the sensitivity of the mechanical system to external sources of vibration, may be quite significant in the field of naval architecture. Analyses varying in complexity are explored and compared with experimental results.

A condition in which hydrofoil oscillatory motion results in low damping without oscillatory instability is defined as "subcritical flutter." Such a condition, which greatly magnifies the sensitivity of the mechanical system to external sources of vibration, may be quite significant in the field of naval architecture. Analyses varying in complexity are explored and compared with experimental results.

A condition in which hydrofoil oscillatory motion results in low damping without oscillatory instability is defined as "subcritical flutter." Such a condition, which greatly magnifies the sensitivity of the mechanical system to external sources of vibration, may be quite significant in the field of naval architecture. Analyses varying in complexity are explored and compared with experimental results.

David Taylor Model Basin. Report 1222.
A CONTROL-SURFACE FLUTTER STUDY IN THE FIELD OF NAVAL ARCHITECTURE, by R.T. McGoldrick and D.A. Jewell. September 1959. v, 45p. illus., photos., graphs, tables, refs. UNCLASSIFIED

This study of control-surface flutter was initiated because of serious hull vibration on destroyers of the DD 931 Class. The source of the vibration had been traced to the twin rudders by the Boston Naval Shipyard.

For making experimental observations on control-surface flutter phenomena in the towing basin, the David Taylor Model Basin constructed the TMB Control-Surface Flutter Apparatus. With this equipment, a marked decrease in overall damping was demonstrated when the downstream mass unbalance was increased during underway tests.

1. Control surfaces – Flutter – Mathematical analysis
2. Control surfaces – Flutter – Test methods
3. Ship hulls – Vibration – Sources
I. McGoldrick, Raymond T.
II. Jewell, David A.
III. NS 715-090

David Taylor Model Basin. Report 1222.
A CONTROL-SURFACE FLUTTER STUDY IN THE FIELD OF NAVAL ARCHITECTURE, by R.T. McGoldrick and D.A. Jewell. September 1959. v, 45p. illus., photos., graphs, tables, refs. UNCLASSIFIED

This study of control-surface flutter was initiated because of serious hull vibration on destroyers of the DD 931 Class. The source of the vibration had been traced to the twin rudders by the Boston Naval Shipyard.

For making experimental observations on control-surface flutter phenomena in the towing basin, the David Taylor Model Basin constructed the TMB Control-Surface Flutter Apparatus. With this equipment, a marked decrease in overall damping was demonstrated when the downstream mass unbalance was increased during underway tests.

1. Control surfaces – Flutter – Mathematical analysis
2. Control surfaces – Flutter – Test methods
3. Ship hulls – Vibration – Sources
I. McGoldrick, Raymond T.
II. Jewell, David A.
III. NS 715-090

David Taylor Model Basin. Report 1222.
A CONTROL-SURFACE FLUTTER STUDY IN THE FIELD OF NAVAL ARCHITECTURE, by R.T. McGoldrick and D.A. Jewell. September 1959. v, 45p. illus., photos., graphs, tables, refs. UNCLASSIFIED

This study of control-surface flutter was initiated because of serious hull vibration on destroyers of the DD 931 Class. The source of the vibration had been traced to the twin rudders by the Boston Naval Shipyard.

For making experimental observations on control-surface flutter phenomena in the towing basin, the David Taylor Model Basin constructed the TMB Control-Surface Flutter Apparatus. With this equipment, a marked decrease in overall damping was demonstrated when the downstream mass unbalance was increased during underway tests.

1. Control surfaces – Flutter – Mathematical analysis
2. Control surfaces – Flutter – Test methods
3. Ship hulls – Vibration – Sources
I. McGoldrick, Raymond T.
II. Jewell, David A.
III. NS 715-090

David Taylor Model Basin. Report 1222.
A CONTROL-SURFACE FLUTTER STUDY IN THE FIELD OF NAVAL ARCHITECTURE, by R.T. McGoldrick and D.A. Jewell. September 1959. v, 45p. illus., photos., graphs, tables, refs. UNCLASSIFIED

This study of control-surface flutter was initiated because of serious hull vibration on destroyers of the DD 931 Class. The source of the vibration had been traced to the twin rudders by the Boston Naval Shipyard.

For making experimental observations on control-surface flutter phenomena in the towing basin, the David Taylor Model Basin constructed the TMB Control-Surface Flutter Apparatus. With this equipment, a marked decrease in overall damping was demonstrated when the downstream mass unbalance was increased during underway tests.

1. Control surfaces – Flutter – Mathematical analysis
2. Control surfaces – Flutter – Test methods
3. Ship hulls – Vibration – Sources
I. McGoldrick, Raymond T.
II. Jewell, David A.
III. NS 715-090

A condition in which hydrofoil oscillatory motion results in low damping without oscillatory instability is defined as "subcritical flutter." Such a condition, which greatly magnifies the sensitivity of the mechanical system to external sources of vibration, may be quite significant in the field of naval architecture. Analyses varying in complexity are explored and compared with experimental results.

A condition in which hydrofoil oscillatory motion results in low damping without oscillatory instability is defined as "subcritical flutter." Such a condition, which greatly magnifies the sensitivity of the mechanical system to external sources of vibration, may be quite significant in the field of naval architecture. Analyses varying in complexity are explored and compared with experimental results.

A condition in which hydrofoil oscillatory motion results in low damping without oscillatory instability is defined as "subcritical flutter." Such a condition, which greatly magnifies the sensitivity of the mechanical system to external sources of vibration, may be quite significant in the field of naval architecture. Analyses varying in complexity are explored and compared with experimental results.

A condition in which hydrofoil oscillatory motion results in low damping without oscillatory instability is defined as "subcritical flutter." Such a condition, which greatly magnifies the sensitivity of the mechanical system to external sources of vibration, may be quite significant in the field of naval architecture. Analyses varying in complexity are explored and compared with experimental results.

David Taylor Model Basin. Report 1222.
A CONTROL-SURFACE FLUTTER STUDY IN THE FIELD OF NAVAL ARCHITECTURE, by R.T. McGoldrick and D.A. Jewell. September 1959. v, 45p. illus., photos., graphs, tables, refs. UNCLASSIFIED

This study of control-surface flutter was initiated because of serious hull vibration on destroyers of the DD 931 Class. The source of the vibration had been traced to the twin rudders by the Boston Naval Shipyard.

For making experimental observations on control-surface flutter phenomena in the towing basin, the David Taylor Model Basin constructed the TMB Control-Surface Flutter Apparatus. With this equipment, a marked decrease in overall damping was demonstrated when the downstream mass unbalance was increased during underway tests.

1. Control surfaces – Flutter – Mathematical analysis
2. Control surfaces – Flutter – Test methods
3. Ship hulls – Vibration – Sources
I. McGoldrick, Raymond T.
II. Jewell, David A.
III. NS 715-090

David Taylor Model Basin. Report 1222.
A CONTROL-SURFACE FLUTTER STUDY IN THE FIELD OF NAVAL ARCHITECTURE, by R.T. McGoldrick and D.A. Jewell. September 1959. v, 45p. illus., photos., graphs, tables, refs. UNCLASSIFIED

This study of control-surface flutter was initiated because of serious hull vibration on destroyers of the DD 931 Class. The source of the vibration had been traced to the twin rudders by the Boston Naval Shipyard.

For making experimental observations on control-surface flutter phenomena in the towing basin, the David Taylor Model Basin constructed the TMB Control-Surface Flutter Apparatus. With this equipment, a marked decrease in overall damping was demonstrated when the downstream mass unbalance was increased during underway tests.

1. Control surfaces – Flutter – Mathematical analysis
2. Control surfaces – Flutter – Test methods
3. Ship hulls – Vibration – Sources
I. McGoldrick, Raymond T.
II. Jewell, David A.
III. NS 715-090

David Taylor Model Basin. Report 1222.
A CONTROL-SURFACE FLUTTER STUDY IN THE FIELD OF NAVAL ARCHITECTURE, by R.T. McGoldrick and D.A. Jewell. September 1959. v, 45p. illus., photos., graphs, tables, refs. UNCLASSIFIED

This study of control-surface flutter was initiated because of serious hull vibration on destroyers of the DD 931 Class. The source of the vibration had been traced to the twin rudders by the Boston Naval Shipyard.

For making experimental observations on control-surface flutter phenomena in the towing basin, the David Taylor Model Basin constructed the TMB Control-Surface Flutter Apparatus. With this equipment, a marked decrease in overall damping was demonstrated when the downstream mass unbalance was increased during underway tests.

1. Control surfaces – Flutter – Mathematical analysis
2. Control surfaces – Flutter – Test methods
3. Ship hulls – Vibration – Sources
I. McGoldrick, Raymond T.
II. Jewell, David A.
III. NS 715-090

David Taylor Model Basin. Report 1222.
A CONTROL-SURFACE FLUTTER STUDY IN THE FIELD OF NAVAL ARCHITECTURE, by R.T. McGoldrick and D.A. Jewell. September 1959. v, 45p. illus., photos., graphs, tables, refs. UNCLASSIFIED

This study of control-surface flutter was initiated because of serious hull vibration on destroyers of the DD 931 Class. The source of the vibration had been traced to the twin rudders by the Boston Naval Shipyard.

For making experimental observations on control-surface flutter phenomena in the towing basin, the David Taylor Model Basin constructed the TMB Control-Surface Flutter Apparatus. With this equipment, a marked decrease in overall damping was demonstrated when the downstream mass unbalance was increased during underway tests.

1. Control surfaces – Flutter – Mathematical analysis
2. Control surfaces – Flutter – Test methods
3. Ship hulls – Vibration – Sources
I. McGoldrick, Raymond T.
II. Jewell, David A.
III. NS 715-090

A condition in which hydrofoil oscillatory motion results in low damping without oscillatory instability is defined as "subcritical flutter." Such a condition, which greatly magnifies the sensitivity of the mechanical system to external sources of vibration, may be quite significant in the field of naval architecture. Analyses varying in complexity are explored and compared with experimental results.

A condition in which hydrofoil oscillatory motion results in low damping without oscillatory instability is defined as "subcritical flutter." Such a condition, which greatly magnifies the sensitivity of the mechanical system to external sources of vibration, may be quite significant in the field of naval architecture. Analyses varying in complexity are explored and compared with experimental results.

A condition in which hydrofoil oscillatory motion results in low damping without oscillatory instability is defined as "subcritical flutter." Such a condition, which greatly magnifies the sensitivity of the mechanical system to external sources of vibration, may be quite significant in the field of naval architecture. Analyses varying in complexity are explored and compared with experimental results.

A condition in which hydrofoil oscillatory motion results in low damping without oscillatory instability is defined as "subcritical flutter." Such a condition, which greatly magnifies the sensitivity of the mechanical system to external sources of vibration, may be quite significant in the field of naval architecture. Analyses varying in complexity are explored and compared with experimental results.